References

[1] Y.M. Ayala, T. Misteli, F.E. Baralle, TDP-43 regulates retinoblastoma protein phosphorylation through the repression of cyclin-dependent kinase 6 expression, Proc. Natl. Acad. Sci. U.S.A. 105 (2008) 3785–3789.

[2] Y.M. Ayala, F. Pagani, F.E. Baralle, TDP43 depletion rescues aberrant CFTR exon 9 skipping, FEBS Lett. 580 (2006) 1339–1344.

[3] E. Buratti, F.E. Baralle, Multiple roles of TDP-43 in gene expression, splicing regulation, and human disease, Front. Biosci. 13 (2008) 867–878.

[4] S.H. Ou, F. Wu, D. Harrich, et al., Cloning and characterization of a novel cellular protein, TDP-43, that binds to human immunodeficiency virus type 1 TAR DNA sequence motifs, J. Virol. 69 (1995) 3584–3596.

[5] I.F. Wang, N.M. Reddy, C.K. Shen, Higher order arrangement of the eukaryotic nuclear bodies, Proc. Natl. Acad. Sci. U.S.A. 99 (2002) 13583–13588.

[6] T. Arai, M. Hasegawa, H. Akiyama, et al., TDP-43 is a component of ubiquitin-positive tau-negative inclusions in frontotemporal lobar degeneration and amyotrophic lateral sclerosis, Biochem. Biophys. Res. Commun. 351 (2006) 602–611.

[7] M. Neumann, D.M. Sampathu, L.K. Kwong, et al., Ubiquitinated TDP-43 in frontotemporal lobar degeneration and amyotrophic lateral sclerosis, Science 314 (2006) 130–133.

[8] T. Arai, I.R. Mackenzie, M. Hasegawa, et al., Phosphorylated TDP-43 in Alzheimer's disease and dementia with Lewy bodies, Acta Neuropathol. (Berl) 117 (2009) 125–136.

[9] M. Hasegawa, T. Arai, H. Akiyama, et al., TDP-43 is deposited in the Guam parkinsonism-dementia complex brains, Brain 130 (2007) 1386–1394.

[10] C.F. Tan, M. Yamada, Y. Toyoshima, et al., Selective occurrence of TDP-43-immunoreactive inclusions in the lower motor neurons in Machado-Joseph disease, Acta Neuropathol. (Berl) 118 (2009) 553–560.

[11] Y. Toyoshima, H. Tanaka, M. Shimohata, et al., Spinocerebellar ataxia type 2 (SCA2) is associated with TDP-43 pathology, Acta Neuropathol. (Berl) 122 (2011) 375–378.

[12] O. Yokota, Y. Davidson, E.H. Bigio, et al., Phosphorylated TDP-43 pathology and hippocampal sclerosis in progressive supranuclear palsy, Acta Neuropathol. (Berl) 120 (2010) 55–66.

[13] E. Kabashi, P.N. Valdmanis, P. Dion, et al., TARDBP mutations in individuals with sporadic and familial amyotrophic lateral sclerosis, Nat. Genet. 40 (2008) 572–574.

[14] J. Sreedharan, I.P. Blair, V.B. Tripathi, et al., TDP-43 mutations in familial and sporadic amyotrophic lateral sclerosis, Science 319 (2008) 1668–1672.

[15] A. Tamaoka, M. Arai, M. Itokawa, et al., TDP-43 M337V mutation in familial amyotrophic lateral sclerosis in Japan, Intern. Med. 49 (2010) 331–334.

[16] I.R. Mackenzie, R. Rademakers, M. Neumann, TDP-43 and FUS in amyotrophic lateral sclerosis and frontotemporal dementia, Lancet Neurol. 9 (2010) 995–1007.

[17] M. Hasegawa, T. Arai, T. Nonaka, et al., Phosphorylated TDP-43 in frontotemporal lobar degeneration and amyotrophic lateral sclerosis, Ann. Neurol. 64 (2008) 60–70.

[18] I.R. Mackenzie, E.H. Bigio, P.G. Ince, et al., Pathological TDP-43 distinguishes sporadic amyotrophic lateral sclerosis from amyotrophic lateral sclerosis with SOD1 mutations, Ann. Neurol. 61 (2007) 427–434.

[19] M. Neumann, L.K. Kwong, A.C. Truax, et al., TDP-43-positive white matter pathology in frontotemporal lobar degeneration with ubiquitin-positive inclusions, J. Neuropathol. Exp. Neurol. 66 (2007) 177–183.

[20] H. Zhang, C.F. Tan, F. Mori, et al., TDP-43-immunoreactive neuronal and glial inclusions in the neostriatum in amyotrophic lateral sclerosis with and without dementia, Acta Neuropathol. (Berl) 115 (2008) 115–122.

[21] M. Neumann, I.R. Mackenzie, N.J. Cairns, et al., TDP-43 in the ubiquitin pathology of frontotemporal dementia with VCP gene mutations, J. Neuropathol. Exp. Neurol. 66 (2007) 152–157.

[22] H.X. Zhang, K. Tanji, F. Mori, et al., Epitope mapping of 2E2-D3, a monoclonal antibody directed against human TDP-43, Neurosci. Lett. 434 (2008) 170–174.

[23] T. Nonaka, F. Kametani, T. Arai, et al., Truncation and pathogenic mutations facilitate the formation of intracellular aggregates of TDP-43, Hum. Mol. Genet. 18 (2009) 3353–3364.

[24] T. Nonaka, T. Arai, E. Buratti, et al., Phosphorylated and ubiquitinated TDP-43 pathological inclusions in ALS and FTLD-U are recapitulated in SH-SY5Y cells, FEBS Lett. 583 (2009) 394–400.

[25] Y. Nishimoto, D. Ito, T. Yagi, et al., Characterization of alternative isoforms and inclusion body of the TAR DNA-binding protein-43, J. Biol. Chem. 285 (2010) 608–619.

[26] E. Buratti, F.E. Baralle, Characterization and functional implications of the RNA binding properties of nuclear factor TDP-43, a novel splicing regulator of CFTR exon 9, J. Biol. Chem. 276 (2001) 36337–36343.

[27] H. Wils, G. Kleinberger, J. Janssens, et al., TDP-43 transgenic mice develop spastic paralysis and neuronal inclusions characteristic of ALS and frontotemporal lobar degeneration, Proc. Natl. Acad. Sci. U.S.A. 107 (2010) 3858–3863.

[28] L.M. Igaz, L.K. Kwong, A. Chen-Plotkin, et al., Expression of TDP-43 C-terminal Fragments in Vitro Recapitulates Pathological Features of TDP-43 Proteinopathies, J. Biol. Chem. 284 (2009) 8516–8524.

[29] M. Hasegawa, T. Nonaka, H. Tsuji, et al., Molecular Dissection of TDP-43 Proteinopathies, J. Mol. Neurosci. 45 (2011) 480–485.

[30] J. Collinge, K.C. Sidle, J. Meads, et al., Molecular analysis of prion strain variation and the aetiology of 'new variant' CJD, Nature 383 (1996) 685–690.

[31] H. Miake, H. Mizusawa, T. Iwatsubo, et al., Biochemical characterization of the core structure of alpha-synuclein filaments, J. Biol. Chem. 277 (2002) 19213–19219.

[32] M. Novak, J. Kabat, C.M. Wischik, Molecular characterization of the minimal protease resistant tau unit of the Alzheimer's disease paired helical filament, EMBO J. 12 (1993) 365–370.

J Mol Neurosci
DOI 10.1007/s12031-011-9571-x

Molecular Dissection of TDP-43 Proteinopathies

Masato Hasegawa · Takashi Nonaka · Hiroshi Tsuji · Akira Tamaoka · Makiko Yamashita · Fuyuki Kametani · Mari Yoshida · Tetsuaki Arai · Haruhiko Akiyama

Received: 30 April 2011 / Accepted: 2 June 2011

Abstract TDP-43 has been identified as a major component of ubiquitin-positive tau-negative cytoplasmic inclusions in frontotemporal lobar degeneration with ubiquitin-positive inclusions (FTLD-U) and in amyotrophic lateral sclerosis (ALS). We raised antibodies to phosphopeptides representing 36 out of 64 candidate phosphorylation sites of human TDP-43 and showed that the antibodies to pS379, pS403/404, pS409, pS410 and pS409/410 labeled the inclusions, but not the nuclei. Immunoblot analyses demonstrated that the antibodies recognized TDP-43 at ~45 kDa, smearing substances and 18–26 kDa C-terminal fragments. Furthermore, the band patterns of the C-terminal fragments differed between neuropathological subtypes, but were indistinguishable between brain regions and spinal cord in each individual patient. Protease treatment of Sarkosyl-insoluble TDP-43 suggests that the different band patterns of the C-terminal fragments reflect different conformations of abnormal TDP-43 molecules between the diseases. These results suggest that molecular species of abnormal TDP-43 are different between the diseases and that they propagate from affected cells to other cells during disease progression and determine the clinicopathological phenotypes of the diseases.

Keywords Propagation · Phosphorylation · Tau · α-Synuclein · Prion · Cancer

M. Hasegawa (✉) · T. Nonaka · H. Tsuji · M. Yamashita · F. Kametani
Department of Neuropathology and Cell Biology,
Tokyo Metropolitan Institute of Medical Science,
2-1-6 Kamikitazawa, Setagaya-ku,
Tokyo 156–8506, Japan
e-mail: hasegawa-ms@igakuken.or.jp

M. Hasegawa · T. Nonaka · M. Yamashita · F. Kametani · T. Arai · H. Akiyama
Dementia Research Project,
Tokyo Metropolitan Institute of Medical Science,
2-1-6 Kamikitazawa, Setagaya-ku,
Tokyo 156–8506, Japan

H. Tsuji · A. Tamaoka
Department of Neurology, Graduate School of Comprehensive Human Sciences, University of Tsukuba,
Ibaraki 305–8577, Japan

M. Yoshida
Department of Neuropathology,
Institute for Medical Science of Aging, Aichi Medical University,
21 Karimata, Yazako, Nagakute-cho, Aichi-gun,
Aichi 480–1195, Japan

T. Arai
Department of Psychiatry, Graduate School of Comprehensive Human Sciences, University of Tsukuba,
Ibaraki 305–8577, Japan

Published online: 16 June 2011

Introduction

TAR DNA-binding protein of M_r=43 kDa (TDP-43) is a nuclear factor that functions in regulating transcription and splicing. It is structurally characterized by two RNA recognition motifs and the C-terminal tail containing a glycine-rich region, and resembles a heterogeneous ribonucleoprotein (hnRNP) (Ayala et al. 2005). It has been shown to interact with several nuclear ribonucleoproteins (RNP), including hnRNP A and B and survival motor neuron protein, inhibiting alternative splicing (Buratti et al. 2005; Bose et al. 2008). In 2006, TDP-43 was identified as a major component of ubiquitin-positive inclusions in frontotemporal lobar degeneration with ubiquitin-positive inclusions (FTLD-U) and amyotrophic lateral sclerosis (ALS) (Arai et al. 2006; Neumann et al. 2006). Subsequent immunohistochemical examination demonstrated abnormal accumulation of TDP-43 in neurodegenerative disorders other than FTLD-U and ALS, including ALS/parkinsonism–

dementia complex of Guam (Geser et al. 2007; Hasegawa et al. 2007), Alzheimer's disease (AD) (Amador-Ortiz et al. 2007; Higashi et al. 2007; Arai et al. 2009), dementia with Lewy bodies (DLB) (Higashi et al. 2007; Nakashima-Yasuda et al. 2007; Arai et al. 2009), Pick's disease (Arai et al. 2006; Freeman et al. 2008; Lin and Dickson 2008), argyrophilic grain disease (Fujishiro et al. 2009) and corticobasal degeneration (Uryu et al. 2008). These diseases with TDP-43 pathologies are now referred to as TDP-43 proteinopathies. In 2008, mutations in the TDP-43 gene (*TARDBP*) were discovered in familial and sporadic cases of ALS (Yokoseki et al. 2008; Gitcho et al. 2008; Sreedharan et al. 2008; Kabashi et al. 2008; Van Deerlin et al. 2008; Barmada and Finkbeiner 2010; Pesiridis et al. 2009), FTD-MND (Benajiba et al. 2009) and FTD (Borroni et al. 2009), clearly indicating that abnormality of TDP-43 protein causes neurodegeneration.

Identification of Abnormal Phosphorylation Sites of TDP-43

Biochemical analyses of the detergent-insoluble fraction extracted from brains of patients afflicted with FTLD-TDP and ALS show that TDP-43 accumulated in these pathological structures is phosphorylated and cleaved (Arai et al. 2006; Neumann et al. 2006). By producing antibodies against synthetic phosphopeptides containing 36 different phosphorylation sites from among the 56 serine/threonine residues of TDP-43, five abnormal phosphorylation sites were identified at serine residues in the C-terminal region (Hasegawa et al. 2008). The antibodies to pS379, pS403/404, pS409, pS410 and pS409/410 strongly stain abnormal neuronal cytoplasmic and dendritic inclusions in FTLD-U, and skein-like and glial cytoplasmic inclusions in ALS spinal cord, with no nuclear staining, and thus permit easier and more sensitive detection of abnormal TDP-43 accumulation in neuropathological examinations (Hasegawa et al. 2008). Immunoblotting of the Sarkosyl-insoluble fraction from control, FTLD-U and ALS cases using these phospho-specific antibodies clearly demonstrated that hyperphosphorylated full-length TDP-43 at ~45 kDa, smearing substances and fragments at 18–26 kDa are the major species of TDP-43 accumulated in FTLD-U and ALS (Hasegawa et al. 2008).

Cellular Models of TDP-43

To establish cellular models of TDP-43 proteinopathies, several deletion mutants of human TDP-43 in SH-SY5Y cells were expressed and the accumulation of TDP-43 was analyzed by use of the phospho-TDP-43 antibodies and ubiquitin. Wild-type (WT) full-length TDP-43 was localized to nuclei and no inclusions were observed, whereas in cells transfected with C-terminal fragments as GFP fusions, round cytoplasmic inclusions with intense GFP fluorescence were formed (Nonaka et al. 2009b). In addition, a deletion mutant lacking the nuclear localizing signal (NLS) and six amino acids similar to the NLS also formed aggregates in cells without any treatment (Nonaka et al. 2009a). These inclusions are strongly positive for antibodies to phosphorylated TDP-43 and ubiquitin. Using these cellular models, the effect of pathogenic mutations of the TDP-43 gene was analyzed. Of 14 mutants examined, seven mutants showed a significantly higher number of aggregates than the WT C-terminal fragment, strongly suggesting that these mutations of TDP-43 accelerate aggregation of the C-terminal fragments (Nonaka et al. 2009b). In addition, when GFP-tagged C-terminal fragments were co-expressed with DsRed-tagged full-length TDP-43, cytoplasmic inclusions with both GFP and DsRed signals were formed, suggesting that exogenous full-length TDP-43 is trapped in cytoplasmic inclusions formed by C-terminal fragments. This may explain why normal nuclear staining of TDP-43 is lost in neuronal cells with inclusions in diseased brains (Nonaka et al. 2009b). Furthermore, we identified two cleavage sites of TDP-43 deposited in FTLD-U by mass spectrometric analysis, and confirmed that expression of these fragments as GFP fusions also afforded cytoplasmic inclusions positive for ubiquitin and phosphorylated TDP-43 (Nonaka et al. 2009b). The cleavage sites identified in the 23-kDa C-terminal fragment of FTLD were different from that of caspase-3, suggesting that caspase is not the enzyme responsible for generating the 23-kDa fragment (Nonaka et al. 2009b). These cellular models recapitulate many of the features of TDP-43 in patients, and therefore, should be useful for screening small molecules for activity to inhibit TDP-43 aggregate formation. We tested whether or not methylene blue and dimebon have the ability to suppress formation of pathological TDP-43 inclusions. Compared to controls, a 50% reduction in the number of inclusions with 0.05 μM methylene blue, a 45% reduction with 5 μM dimebon and an 80% reduction with the combination of 0.05 μM methylene blue and 5 μM dimebon were observed (Yamashita et al. 2009). The effects were statistically significant and the results were also confirmed by Western blotting. These results suggest that these two compounds may be effective in the therapy of ALS, FTLD-U and other TDP-43 proteinopathies.

TDP-43 C-Terminal Fragments

Based on neuropathological studies, TDP-43 proteinopathies have been classified into 4 subtypes (Cairns et al.

2007). Type 1 is characterized by dystrophic neurites (DNs) with few neuronal cytoplasmic inclusions (NCIs) and no neuronal intranuclear inclusions (NIIs), Type 2 has numerous NCIs with few DNs and no NIIs, Type 3 has numerous NCIs and DNs and occasional NIIs and Type 4 has numerous NIIs and DNs with few NCIs, a pattern which is specific for familial FTLD-U with mutations of VCP gene. There appears to be a strong relationship between other subtypes of TDP-43 pathology and clinical phenotype. Type 1 is associated with semantic dementia, type 2 with FTLD with motor neuron disease (MND), ALS or clinical signs of MND, and type 3 with progressive non-fluent aphasia or FTD with mutation in the progranulin gene. Recent studies of ALS have clarified the wide distribution of neuronal and glial TDP-43 pathology in multiple areas of the central nervous systems (Geser et al. 2008; Nishihira et al. 2009), suggesting that ALS does not selectively affect only the motor system, but rather is a multisystem neurodegenerative TDP-43 proteinopathy affecting both neurons and glial cells.

By immunoblot analyses of the Sarkosyl-insoluble fractions from FTLD-U and ALS patients, we found that the band patterns of the C-terminal fragments of phosphorylated TDP-43 corresponded to the neuropathological subtypes. Type 1 FTLD-U showed two major bands at 23 and 24 kDa and two minor bands at 18 and 19 kDa, while type 2 ALS showed three major bands at 23, 24 and 26 kDa and two minor bands at 18 and 19 kDa. Type 3 FTD with mutation in the progranulin gene showed an intermediate pattern between those two. These results clearly indicate that TDP-43 proteinopathies subclassified by neuropathological differences can also be distinguished biochemically. This strong association between the neuropathology and the biochemistry is critical for understanding the molecular pathogenesis of TDP-43 proteinopathies.

Biochemical Analysis of TDP-43 in FTLD-U and ALS

The biochemical differences of TDP-43, as shown in the different band patterns of TDP-43 C-terminal fragments, are closely linked to the morphologies of inclusions. The properties of the abnormal TDP-43 may determine the neuropathological and clinical phenotypes of TDP-43 proteinopathies. Similar biochemical and neuropathological differences have been reported in tau between PSP and CBD. Both PSP and CBD are tauopathies with deposition of 4-repeat tau isoforms; however, distinct types of C-terminal fragments are detected, i.e., a 33-kDa band in PSP and ~3-kDa bands in CBD (Arai et al. 2004).

So, what do the different band patterns mean? It is clear that the fragments are produced by cleavage at multiple sites of TDP-43. The band patterns also suggest that the cleavage sites are slightly altered between the diseases. Based on these observations, it is likely that the event may occur after the assembly or aggregation of abnormal TDP-43, and represent relatively protease-resistant domains of TDP-43, which form beta-sheet structure. That is, the different band patterns in TDP-43 proteinopathies represent different conformations of abnormal TDP-43 in the diseases.

To test this idea, we performed protease treatment of the abnormal TDP-43 recovered in the Sarkosyl-insoluble pellets, and analyzed the protease-resistant bands. Proteins can be easily cleaved by proteases if they are denatured or unstructured, but domains that have rigid structures such as beta-sheet structure, or that are structurally buried or interacting with other molecules, are highly resistant to proteases. Figure 1 shows the result of immunoblot analysis of abnormal TDP-43 from two ALS and two FTLD-U cases before and after protease treatment. Before treatment, hyperphosphorylated full-length TDP-43 at 45 kDa, smearing substances and 18–26 kDa C-terminal fragments were detected by pS409/410. The band patterns of the C-terminal fragments are different between FTLD-U with type 1 pathology and ALS with type 2 pathology. Upon trypsin or chymotrypsin treatment, the full-length 45-kDa band and smearing substance of TDP-43 disappeared and protease-resistant core fragments appeared at 16–26 kDa (Fig. 1). As expected, the protease-resistant band pattern of ALS is different and clearly distinguishable from that of FTLD-U. Doublet bands at ~16 kDa and a band at 25 kDa were detected in ALS, but only a single broad band at ~16 kDa was detected in FTLD-U with type 1 pathology after trypsin treatment (Fig. 1). Similarly, multiple protease-resistant bands were detected at 16–25 kDa after chymotrypsin treatment and the band patterns were different between ALS and FTLD-U (Fig. 1). These results strongly support the idea that the different band patterns of the C-terminal fragments reflect different conformations of abnormal TDP-43 molecules between ALS and FTLD-U.

TDP-43 in Different Brain Regions

Similar protease-resistant bands and differences in the band patterns have been reported in prion diseases, CJD and BSE (Collinge et al. 1996). Protease-resistant prion from new-variant CJD cases showed a different characteristic pattern from that in sporadic CJD cases, and the band pattern is indistinguishable from that of mice infected with BSE prion. This is biochemical evidence that the BSE agent has been transmitted from bovine to human.

Applying this to TDP-43 in TDP-43 proteinopathies, it is possible to determine whether there is any difference between the abnormal TDP-43 accumulated in cortex and that in spinal cord by analyzing the band patterns of the C-

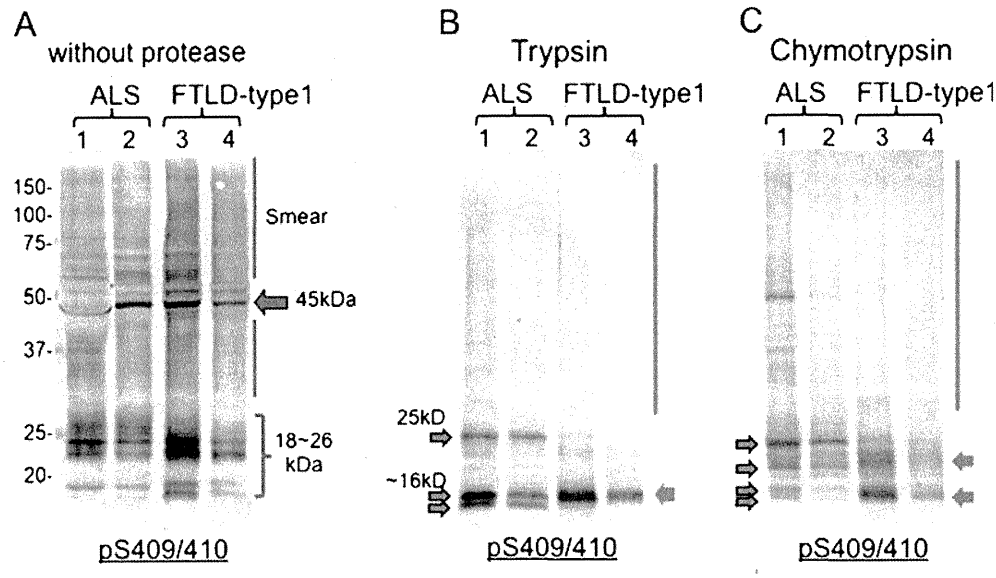

Fig. 1 Immunoblot analysis of abnormal TDP-43 from two ALS and two FTLD-U cases before and after protease treatment with a phosphorylation dependent anti-TDP-43 rabbit polyclonal antibody (pS409/410). **a** Hyperphosphorylated full-length TDP-43 at 45 kDa, smearing substances and 18–26 kDa C-terminal fragments were detected by pS409/410 before treatment. The band patterns of the C-terminal fragments are different between FTLD-U with type 1 pathology and ALS with type 2 pathology. **b** Upon trypsin treatment, the full-length 45 kDa band and smearing substance of TDP-43 disappeared and protease-resistant core fragments appeared at 16~26 kDa. Doublet bands at ~16 kDa and a band at 25 kDa were seen in ALS, but a single broad band at ~16 kDa was detected in FTLD-U with type 1 pathology after trypsin treatment. **c** Multiple protease-resistant bands were detected at 16~25 kDa after chymotrypsin treatment and the band patterns were different between ALS and FTLD-U

terminal fragments of TDP-43. Thus, we have prepared Sarkosyl-insoluble fractions from cortex and spinal cords of three ALS cases, immunoblotted them with pS409/410 and compared the results. In all three cases, type 2 C-terminal fragments of TDP-43 were detected, and there was no significant difference between the band pattern in cortex and that in spinal cord (data not shown). This strongly suggests that the same form of abnormal TDP-43 molecule is deposited in different brain regions. Similar results were also obtained from the analysis of the C-terminal band pattern of TDP-43 in FTLD-U. It seems highly unlikely that the same conformational change would occur synchronously in different brain regions. Instead, it seems more likely that abnormal protein produced in cells is transferred to different regions and propagated. These biochemical data obtained from the brains of patients provide biochemical evidence that abnormal species of TDP-43 are transmitted from cell to cell and propagated in vivo.

Discussion

Amyloid-like protein deposition is a common neuropathological feature of many neurodegenerative diseases. Hyperphosphorylated tau in Alzheimer's disease and related tauopathies, hyperphosphorylated alpha-synuclein in Parkinson's disease and other alpha-synucleinopathies, and expanded polyglutamines in polyglutamine diseases have been identified. Importantly, the extent of the abnormal protein pathologies is closely correlated with the disease progression (Braak and Braak 1991; Braak et al. 2003; Saito et al. 2003). The proteins or protein fibrils deposited in cells in these diseases have been shown to have a common structural feature. Cross-beta structure, which is the same as in abnormal prion protein, has been demonstrated in filaments or fibrils composed of tau (Berriman et al. 2003), alpha-synuclein (Serpell et al. 2000) or expanded polyglutamines (Perutz 1999). It has not been demonstrated in TDP-43 yet, but we have shown by electron microscopy that phosphorylated TDP-43 in motor neurons of ALS patients has a fibrous structure (Hasegawa et al. 2008), suggesting that TDP-43 is also an amyloid-like protein.

For the assembly of amyloid fibrils, nucleation-dependent protein polymerization has been proposed. This comprises nucleation and elongation phases, and nucleation is the rate-limiting step. It takes a long time to form the first aggregated seed from the monomer, but once the seed is formed, the elongation step proceeds relatively quickly. More importantly, by addition of amyloid-seed, proteins are often converted to the same conformation as that of the seed. For example, WT monomeric alpha-synuclein is converted to A30P-type amyloid fibrils when it is incubated with a small amount of fibril-seeds formed with A30P mutant alpha-synuclein (Yonetani et al. 2009). Differences in the conformations of the amyloid fibrils are detected based on the differences in the protease-resistant band

patterns, as in the typing of prion proteins. There is another example of nucleation-dependent amyloid fibril formation in cultured cells. We developed a novel method for introducing amyloid seeds into cultured cells using lipofectoamine, and presented experimental evidence of seed-dependent polymerization of alpha-synuclein, leading to the formation of filamentous protein deposits and cell death (Nonaka et al. 2010). Overexpression of alpha-synuclein itself in cells does not generate abnormal inclusions, but if fibril seeds formed with alpha-synuclein are introduced into cells, abundant filamentous alpha-synuclein aggregates positive for PSer129 and ubiquitin are developed, and cells with inclusions undergo cell death. This was also clearly demonstrated in cells expressing different tau isoforms by introducing the corresponding tau fibril seeds (Nonaka et al. 2010).

The above results obtained from biochemical analyses of abnormal proteins in patients strongly suggest that intracellular amyloid-like proteins, including TDP-43, propagate from cell to cell and this propagation is the cause of disease progression, analogously to metastasis of cancer cells to multiple different tissues in cancer progression. From this point of view, we have proposed as a hypothesis that neurodegenerative diseases with amyloid-like proteins can be regarded as "protein cancers." The term prion, coined in 1982 by Stanley B. Prusiner, describes an agent transmissible among humans and a variety of mammals. On the other hand, the term "protein cancers" describes diseases that involve the spreading or propagation of abnormal proteins in tissues or individuals, even though the mechanism of propagation is basically the same as that of prions. Amyloid-like protein interacts with normal protein and converts it to the same abnormal conformation, and the amplified amyloid-like protein is transmitted from cell to cell, probably through synapses, and propagates to various brain regions (Fig. 2). As a result, the same abnormal protein pathology expands gradually, and clinical manifestations that are associated with affected brain regions become more marked because of the transmission and propagation of the abnormal protein. Therefore, it is important to regulate the propagation of abnormal proteins for clinical therapy.

Conclusions

1. In ALS, FTLD-U and other TDP-43 proteinopathies, abnormally phosphorylated, ubiquitinated, and truncated TDP-43 is accumulated in a filamentous form.
2. We established cellular models which recapitulate many of the features of the abnormal TDP-43 in FTLD-U and ALS
3. ALS-related pathogenic mutations of the TDP-43 gene accelerate aggregate formation by the C-terminal fragments.
4. The band pattern of the TDP-43 C-terminal fragments is different between diseases with different clinicopathological phenotypes, and it represents different conformations of the abnormal TDP-43 between the diseases.
5. The C-terminal band patterns in several brain areas and spinal cord in each individual case of sporadic ALS are indistinguishable.
6. These and other results suggest that abnormal TDP-43, tau and alpha-synuclein are transmitted and propagated from cell to cell in different regions during disease progression. It is important to find drugs that can block the propagation of abnormal proteins for clinical therapy.

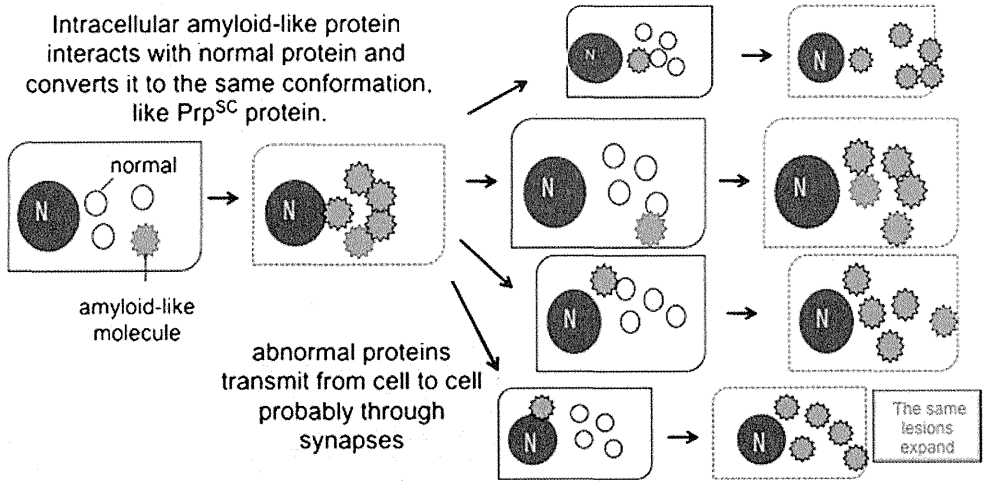

Fig. 2 Schematic representation of prion-like conversion of normal protein into amyloid-like protein and its propagation in neurodegenerative diseases. Intracellular amyloid-like protein interacts with normal protein and converts it to the same abnormal conformation. Amplified abnormal amyloid-like protein is transmitted from cell to cell, probably through synapses, and propagates to various brain regions. As a result, the same abnormal protein pathology expands gradually, and clinical manifestations that are associated with affected brain regions become more marked because of the transmission and propagation of the abnormal protein. From this point of view, neurodegenerative diseases with amyloid-like proteins can be regarded as 'protein cancers"

References

Amador-Ortiz C, Lin WL, Ahmed Z et al (2007) TDP-43 immunoreactivity inhippocampal sclerosis and Alzheimer's disease. Ann Neurol 61:435–445

Arai T, Ikeda K, Akiyama H, Nonaka T, Hasegawa M, Ishiguro K et al (2004) Identification of amino-terminally cleaved tau fragments that distinguish progressive supranuclear palsy from corticobasal degeneration. Ann Neurol 55:72–79

Arai T, Hasegawa M, Akiyama H et al (2006) TDP-43 is a component of ubiquitin-positive tau-negative inclusions in frontotemporal lobar degeneration and amyotrophic lateral sclerosis. Biochem Biophys Res Commun 351:602–611

Arai T, Mackenzie IR, Hasegawa M et al (2009) Phosphorylated TDP-43 in Alzheimer's disease and dementia with Lewy bodies. Acta Neuropathol 117:125–136

Ayala YM, Pantano S, D'Ambrogio A et al (2005) Human, *Drosophila*, and *C. elegans* TDP43: nucleic acid binding properties and splicing regulatory function. J Mol Biol 348:575–588

Barmada SJ, Finkbeiner S (2010) Pathogenic TARDBP mutations in amyotrophic lateral sclerosis and frontotemporal dementia: disease-associated pathways. Rev Neurosci 21:251–272 (Review)

Benajiba L, Le Ber I, Camuzat A, Lacoste M et al (2009) TARDBP mutations in motoneuron disease with frontotemporal lobar degeneration. Ann Neurol 65:470–473

Berriman J, Serpell LC, Oberg KA et al (2003) Tau filaments from human brain and from in vitro assembly of recombinant protein show cross-beta structure. Proc Natl Acad Sci USA 100:9034–9038

Borroni B, Bonvicini C, Alberici A et al (2009) Mutation within TARDBP leads to frontotemporal dementia without motor neuron disease. Hum Mutat 30:E974–E983

Bose JK, Wang IF, Hung L, Tarn WY, Shen CK (2008) TDP-43 overexpression enhances exon 7 inclusion during the survival of motor neuron pre-mRNA splicing. J Biol Chem 283:28852–28859

Braak H, Braak E (1991) Neuropathological staging of Alzheimer-related changes. Acta Neuropathol 82:239–259

Braak H, Del Tredici K, Rub U, de Vos RA et al (2003) Staging of brain pathology related to sporadic Parkinson's disease. Neurobiol Aging 24:197–211

Buratti E, Brindisi A, Giombi M, Tisminetzky S, Ayala YM, Baralle FE (2005) TDP-43 binds heterogeneous nuclear ribonucleoprotein A/B through its C-terminal tail. J Biol Chem 280:37572–37584

Cairns NJ, Bigio EH, Mackenzie IR et al (2007) Neuropathologic diagnostic and nosologic criteria for frontotemporal lobar degeneration: consensus of the Consortium for Frontotemporal Lobar Degeneration. Acta Neuropathol 114:5–22

Collinge J, Sidle KC, Meads J, Ironside J, Hill AF (1996) Molecular analysis of prion strain variation and the aetiology of 'new variant' CJD. Nature 383:685–690

Freeman SH, Spires-Jones T, Hyman BT, Growdon JH, Frosch MP (2008) TAR-DNA binding protein 43 in Pick disease. J Neuropathol Exp Neurol 67:62–67

Fujishiro H, Uchikado H, Arai T et al (2009) Accumulation of phosphorylated TDP-43 in brains of patients with argyrophilic grain disease. Acta Neuropathol 117:151–158

Geser F, Winton MJ, Kwong LK et al (2007) Pathological TDP-43 in parkinsonism-dementia complex and amyotrophic lateral sclerosis of Guam. Acta Neuropathol 115:133–145

Geser F, Brandmeir NJ, Kwong LK et al (2008) Evidence of multisystem disorder in whole-brain map of pathological TDP-43 in amyotrophic lateral sclerosis. Arch Neurol 65:636–641

Gitcho MA, Baloh RH, Chakraverty S et al (2008) TDP-43 A315T mutation in familial motor neuron disease. Ann Neurol 63:535–538

Hasegawa M, Arai T, Akiyama H et al (2007) TDP-43 is deposited in the Guam parkinsonism-dementia complex brains. Brain 130:1386–1394

Hasegawa M, Arai T, Nonaka T et al (2008) Phosphorylated TDP-43 in frontotemporal lobar degeneration and amyotrophic lateral sclerosis. Ann Neurol 64:60–70

Higashi S, Iseki E, Yamamoto R et al (2007) Concurrence of TDP-43, tau and alpha-synuclein pathology in brains of Alzheimer's disease and dementia with Lewy bodies. Brain Res 1184:284–294

Kabashi E, Valdmanis PN, Dion P et al (2008) TARDBP mutations in individuals with sporadic and familial amyotrophic lateral sclerosis. Nat Genet 40:572–574

Lin WL, Dickson DW (2008) Ultrastructural localization of TDP-43 in filamentous neuronal inclusions in various neurodegenerative diseases. Acta Neuropathol 116:205–213

Nakashima-Yasuda H, Uryu K, Robinson J et al (2007) Co-morbidity of TDP-43 proteinopathy in Lewy body related diseases. Acta Neuropathol 114:221–229

Neumann M, Sampathu DM, Kwong LK et al (2006) Ubiquitinated TDP-43 in frontotemporal lobar degeneration and amyotrophic lateral sclerosis. Science 314:130–133

Nishihira Y, Tan CF, Hoshi Y et al (2009) Sporadic amyotrophic lateral sclerosis of long duration is associated with relatively mild TDP-43 pathology. Acta Neuropathol 117:45–53

Nonaka T, Arai T, Buratti E, Baralle FE, Akiyama H, Hasegawa M (2009a) Phosphorylated and ubiquitinated TDP-43 pathological inclusions in ALS and FTLD-U are recapitulated in SH-SY5Y cells. FEBS Lett 583:394–400

Nonaka T, Kametani F, Arai T, Akiyama H, Hasegawa M (2009b) Truncation and pathogenic mutations facilitate the formation of intracellular aggregates of TDP-43. Hum Mol Genet 18:3353–3364

Nonaka T, Watanabe ST, Iwatsubo T, Hasegawa M (2010) Seeded aggregation and toxicity of alpha-synuclein and tau: cellular models of neurodegenerative diseases. J Biol Chem 285:34885–34898

Perutz MF (1999) Glutamine repeats and neurodegenerative diseases. Brain Res Bull 50:467

Pesiridis GS, Lee VM, Trojanowski JQ (2009) Mutations in TDP-43 link glycine-rich domain functions to amyotrophic lateral sclerosis. Hum Mol Genet 18:R156–R162

Saito Y, Kawashima A, Ruberu NN, Fujiwara H et al (2003) Accumulation of phosphorylated alpha-synuclein in aging human brain. J Neuropathol Exp Neurol 62:644–654

Serpell LC, Berriman J, Jakes R et al (2000) Fiber diffraction of synthetic alpha-synuclein filaments shows amyloid-like cross-beta conformation. Proc Natl Acad Sci USA 97:4897–4902

Sreedharan J, Blair IP, Tripathi VB et al (2008) TDP-43 mutations in familial and sporadic amyotrophic lateral sclerosis. Science 319:1668–1672

Uryu K, Nakashima-Yasuda H, Forman MS et al (2008) Concomitant TAR-DNA-binding protein 43 pathology is present in Alzheimer disease and corticobasal degeneration but not in other tauopathies. J Neuropathol Exp Neurol 67:555–564

Van Deerlin VM, Leverenz JB, Bekris LM et al (2008) TARDBP mutations in amyotrophic lateral sclerosis with TDP-43 neuropathology: a genetic and histopathological analysis. Lancet Neurol 7:409–416

Yamashita, M., Nonaka, T., Arai, T et al (2009) Methylene blue and dimebon inhibit aggregation of TDP-43 in cellular models. FEBS Lett 583:2419–24

Yokoseki A, Shiga A, Tan CF et al (2008) TDP-43 Mutation in familial amyotrophic lateral sclerosis. Ann Neurol 63:538–542

Yonetani M, Nonaka T, Masuda M et al (2009) Conversion of wild-type alpha-synuclein into mutant-type fibrils and its propagation in the presence of A30P mutant. J Biol Chem 284:7940–7950

THE JOURNAL OF BIOLOGICAL CHEMISTRY VOL. 285, NO. 45, pp. 34885–34898, November 5, 2010

Seeded Aggregation and Toxicity of α-Synuclein and Tau

CELLULAR MODELS OF NEURODEGENERATIVE DISEASES[*][S]

Received for publication, May 26, 2010, and in revised form, August 17, 2010 Published, JBC Papers in Press, August 30, 2010, DOI 10.1074/jbc.M110.148460

Takashi Nonaka[‡1], **Sayuri T. Watanabe**[‡§], **Takeshi Iwatsubo**[§¶], **and Masato Hasegawa**[‡2]

From the [‡]*Department of Molecular Neurobiology, Tokyo Institute of Psychiatry, Tokyo 156-8585 and the* [§]*Department of Neuropathology and Neuroscience, Graduate School of Pharmaceutical Science, and* [¶]*Department of Neuropathology, Graduate School of Medicine, University of Tokyo, Tokyo 113-0033, Japan*

The deposition of amyloid-like filaments in the brain is the central event in the pathogenesis of neurodegenerative diseases. Here we report cellular models of intracytoplasmic inclusions of α-synuclein, generated by introducing nucleation seeds into SH-SY5Y cells with a transfection reagent. Upon introduction of preformed seeds into cells overexpressing α-synuclein, abundant, highly filamentous α-synuclein-positive inclusions, which are extensively phosphorylated and ubiquitinated and partially thioflavin-positive, were formed within the cells. SH-SY5Y cells that formed such inclusions underwent cell death, which was blocked by small molecular compounds that inhibit β-sheet formation. Similar seed-dependent aggregation was observed in cells expressing four-repeat Tau by introducing four-repeat Tau fibrils but not three-repeat Tau fibrils or α-synuclein fibrils. No aggregate formation was observed in cells overexpressing three-repeat Tau upon treatment with four-repeat Tau fibrils. Our cellular models thus provide evidence of nucleation-dependent and protein-specific polymerization of intracellular amyloid-like proteins in cultured cells.

The conversion of certain soluble peptides and proteins into insoluble filaments or misfolded amyloid proteins is believed to be the central event in the etiology of a majority of neurodegenerative diseases (1–4). Alzheimer disease (AD)[3] is characterized by the deposition of two kinds of filamentous aggregates, extracellular deposits of β-amyloid plaques composed of amyloid β (Aβ) peptides, and intracellular neurofibrillary lesions consisting of hyperphosphorylated Tau. In Parkinson disease (PD) and dementia with Lewy bodies (DLB), filamentous inclusions consisting of hyperphosphorylated α-synuclein (α-syn) are accumulated in degenerating neurons (5). The deposition of prion proteins in synapses and extracellular spaces is the defining characteristic of Creutzfeldt-Jakob disease and other prion diseases (3). The identification of genetic defects associated with early onset AD, familial PD, frontotemporal dementia, parkinsonism linked to chromosome 17 (caused by Tau mutation and deposition), and familial Creutzfeldt-Jakob disease has led to the hypothesis that the production and aggregation of these proteins are central to the development of neurodegeneration. Fibrils formed of Aβ display a prototypical cross-β-structure characteristic of amyloid (6), as do many other types of filaments deposited in the extracellular space in systemic or organ-specific amyloidoses (7), including prion protein deposits (8). Filaments assembled from α-syn (9) and from Tau filaments (10) were also shown to possess cross-β-structure, as were synthetic filaments derived from exon 1 of huntingtin with 51 glutamines (11). It therefore seems appropriate to consider neurodegenerative disorders developing intracellular deposits of amyloid-like proteins as brain amyloidosis. The accumulation and propagation of extracellular amyloid proteins are believed to occur through nucleation-dependent polymerization (12, 13). However, it has been difficult to establish the relevance of this process in the *in vivo* situation because of the lack of a suitable cell culture model or method to effectively introduce seeds into cells. For example, it has not yet been possible to generate *bona fide* fibrous inclusions reminiscent of Lewy bodies as a model of PD by overexpressing α-syn in neurons of transgenic animals. Here, we describe a novel method for introducing amyloid seeds into cultured cells using lipofection, and we present experimental evidence of seed-dependent polymerization of α-syn, leading to the formation of filamentous protein deposits and cell death. This was also clearly demonstrated in cells expressing different Tau isoforms by introducing the corresponding Tau fibril seeds.

EXPERIMENTAL PROCEDURES

Chemicals and Antibodies—A phosphorylation-independent antibody Syn102 and monoclonal and polyclonal antibodies against a synthetic phosphopeptide of α-syn (Ser(P)[129]) were used as described previously (5). Polyclonal anti-ubiquitin antibody was obtained from Dako. Polyclonal anti-Tau Ser(P)[396] was obtained from Calbiochem. Monoclonal anti-α-tubulin and anti-HA clone HA-7 were obtained from Sigma. Lipofectamine was purchased from Invitrogen. Monoclonal

* This work was supported by grants-in-aid for scientific research on Priority Areas, Research on Pathomechanisms of Brain Disorders (to T. I. and M. H.) and Grant-in-aid for Scientific Research (C) 19590297 and 22500345 (to T. N.) from the Ministry of Education, Culture, Sports, Science, and Technology of Japan.

[S] The on-line version of this article (available at http://www.jbc.org) contains supplemental Figs. S1–S5.

[1] To whom correspondence may be addressed: Dept. of Molecular Neurobiology, Tokyo Institute of Psychiatry 2-1-8 Kamikitazawa, Setagaya-ku, Tokyo 156-8585, Japan. Tel.: 81-3-3304-5701; Fax: 81-3-3329-8035; E-mail: nonaka-tk@igakuken.or.jp.

[2] To whom correspondence may be addressed: Dept. of Molecular Neurobiology, Tokyo Institute of Psychiatry 2-1-8 Kamikitazawa, Setagaya-ku, Tokyo 156-8585, Japan. Tel.: 81-3-3304-5701; Fax: 81-3-3329-8035; E-mail: hasegawa-ms@igakuken.or.jp.

[3] The abbreviations used are: AD, Alzheimer disease; Aβ, amyloid β; PD, Parkinson disease; DLB, dementia with Lewy bodies; α-syn, α-synuclein; 3R1N, three-repeat Tau isoform with one amino-terminal insert; 4R1N, four-repeat Tau isoform with one amino-terminal insert; LA, Lipofectamine; LDH, lactate dehydrogenase.

anti-Tau T46 was from Zymed Laboratories Inc.. AT100 and HT7 antibodies were obtained from Innogenetics.

Preparation of α-Syn Seed, Oligomers, and Tau Fibrils—Human α-syn cDNA in bacterial expression plasmid pRK172 was used to produce recombinant protein (14). Wild-type (WT) or carboxyl-terminally HA-tagged α-syn was expressed in *Escherichia coli* BL21 (DE3) and purified as described (15). To obtain α-syn fibrils, α-syn (5–10 mg/ml) was incubated at 37 °C for 4 days with continuous shaking. The samples were diluted with 5 volumes of 30 mM Tris-HCl buffer (pH 7.5) and ultracentrifuged at 110,000 × *g* for 20 min at 25 °C. The pellets were resuspended in 30 mM Tris-HCl buffer (pH 7.5) and sonicated twice for 5 s each. The protein concentration was determined as described, and this preparation was used as Seed αS. In the case of α-syn oligomers, α-syn (10 mg/ml) was incubated at 37 °C for 3 days in the presence of 10 mM exifone. After incubation, the mixture was ultracentrifuged at 110,000 × *g* for 20 min at 25 °C. The supernatant was desalted by Sephadex G-25 (Amersham Biosciences) column chromatography, and eluted fractions (α-syn oligomers) were analyzed by reversed-phase HPLC, SDS-PAGE, and immunoblot analysis. Recombinant human three-repeat Tau isoform with one amino-terminal insert (3R1N) and four-repeat Tau isoform with one amino-terminal insert (4R1N) monomer and corresponding fibrils were prepared as described previously (16, 17).

Introduction of Proteins into Cells—Human neuroblastoma SH-SY5Y cells obtained from ATCC were cultured in DMEM/F-12 medium with 10% FCS. Cells at ~30–50% confluence in 6-well plates were treated with 200 μl of Opti-MEM containing 2 μg of the seed α-syn WT (Seed αS); HA-tagged α-syn (Seed-HA); α-syn monomers, oligomers; or Tau 3R1N or 4R1N fibrils; and 5 μl of Lipofectamine (LA) for 3 h at 37 °C. The medium was changed to DMEM/F-12, and culture was continued for 14 h. The cells were collected by treatment with 0.5 ml of 0.25% trypsin for 10 min at 37 °C, followed by centrifugation (1,800 × *g*, 5 min) and washing with PBS. The cellular proteins were extracted with 100 μl of homogenization buffer containing 50 mM Tris-HCl, pH 7.5, 0.15 M NaCl, 5 mM EDTA, and a mixture of protease inhibitors by sonication. After ultracentrifugation at 290,000 × *g* for 20 min at 4 °C, the supernatant was collected as a Tris-soluble fraction, and the protein concentration was determined by BCA assay. The pellet was solubilized in 100 μl of SDS-sample buffer. Both Tris-soluble and insoluble fractions were analyzed by immunoblotting with appropriate antibodies as indicated (15, 18).

Cell Culture Model of Seed-dependent Polymerization of α-Syn or Tau—α-Syn or Tau 3R1N or 4R1N was transiently overexpressed in SH-SY5Y cells by transfection of 1 μg of wild-type human α-syn cDNA in pcDNA3 (pcDNA3-α-syn) or human Tau cDNA in pcDNA3 (pcDNA3-Tau 3R1N or 4R1N) with 3 μl of FuGENE6 (Roche Applied Science) in 100 μl of Opti-MEM, followed by culture for 14 h. Under our experimental conditions, the efficiency of transfection with pEGFP-C1 vector was 20–30%. The cells were washed with PBS once, and then Seed αS, Seed-HA, Seed 3R1N, or Seed 4R1N was introduced with Lipofectamine as described above. The medium was changed to DMEM/F-12, and culture was continued for ~2–3 days. Cells were harvested in the presence of trypsin to digest extracellular cell-associated α-syn fibrils. The cellular proteins were differentially extracted and immunoblotted with the indicated antibodies, as described (18).

Confocal Microscopy—SH-SY5Y cells on coverslips were transfected with pcDNA3-α-syn and cultured for 14 h as described above, and then Seed αS was introduced, and culture was continued for ~1–2 days. After fixation with 4% paraformaldehyde, the cells were stained with appropriate primary and secondary antibodies as described previously (18). For thioflavin S staining, the cells were incubated with 0.05% thioflavin S at room temperature for 5 min. Fluorescence was analyzed with a laser-scanning confocal fluorescence microscope (LSM5Pascal, Carl Zeiss).

Immunoelectron Microscopy—For electron microscopy, cells overexpressing α-syn were transfected with Seed αS, cultured for 2 days, fixed in 0.1 M phosphate buffer containing 4% glutaraldehyde for 12 h, and then processed and embedded in LR White resin (London Resin, Reading, UK). Ultrathin sections were stained with uranyl acetate for investigation. Immunolabeling of the inclusions was performed by means of an immunogold-based postembedding procedure. Sections were blocked with 10% calf serum, incubated overnight on grids with anti-Ser(P)^{129} antibody at a dilution of 1:100, rinsed, then reacted with secondary antibody conjugated to 10-nm gold particles (E-Y Laboratories, San Mateo, CA) (1:10), rinsed again and stained with uranyl acetate.

Immunoelectron microscopic analysis of α-syn or Tau filaments extracted from cells was performed as follows. Cells overexpressing α-syn or Tau were transfected with Seed αS or Seed Tau, respectively. After incubation for 3 days, they were harvested, suspended in 200 μl of 10 mM Tris-HCl, pH 7.4, 1 mM EGTA, 10% sucrose, 0.8 M NaCl) and sonicated. The lysates were centrifuged at 20,400 × *g* for 20 min at 4 °C. The supernatant was recovered, and Sarkosyl was added (final 1%, v/v). The mixtures were incubated at room temperature for 30 min and then centrifuged at 113,000 × *g* for 20 min. The resulting pellets were suspended in 30 mM Tris-HCl, pH 7.5, placed on collodion-coated 300-mesh copper grids, and stained with the indicated antibodies and 2% (v/v) phosphotungstate. Micrographs were recorded on a JEOL 1200EX electron microscope.

Cell Death Assay—Cell death assay was performed using a CytoTox 96 non-radioactive cytotoxicity assay kit (Promega). TUNEL staining was performed using an *in situ* cell death detection kit (Roche Applied Science).

Assay of Proteasome Activity—SH-SY5Y cells transfected with pcDNA3-α-syn and Seed αS were cultured for 3 days or treated with 20 μM MG132 for 4 h. Cells were harvested, and cytosolic fraction was prepared as follows. Cells were resuspended in 100 μl of phosphate-buffered saline (PBS) and disrupted by sonication, and then insoluble material was removed by ultracentrifugation at 290,000 × *g* for 20 min at 4 °C. The supernatant was assayed for proteasome activity by using a fluorescent peptide substrate, benzyloxycarbonyl-Leu-Leu-Glu-7-amido-4-methylcoumarin (Peptide Institute, Inc.). 7-Amino-4-methylcoumarin release was measured fluorometrically (excitation at 365 nm; emission at 460 nm). In a green fluorescent protein (GFP) reporter assay of proteasome activity in living cells by confocal laser microscopy, SH-SY5Y cells trans-

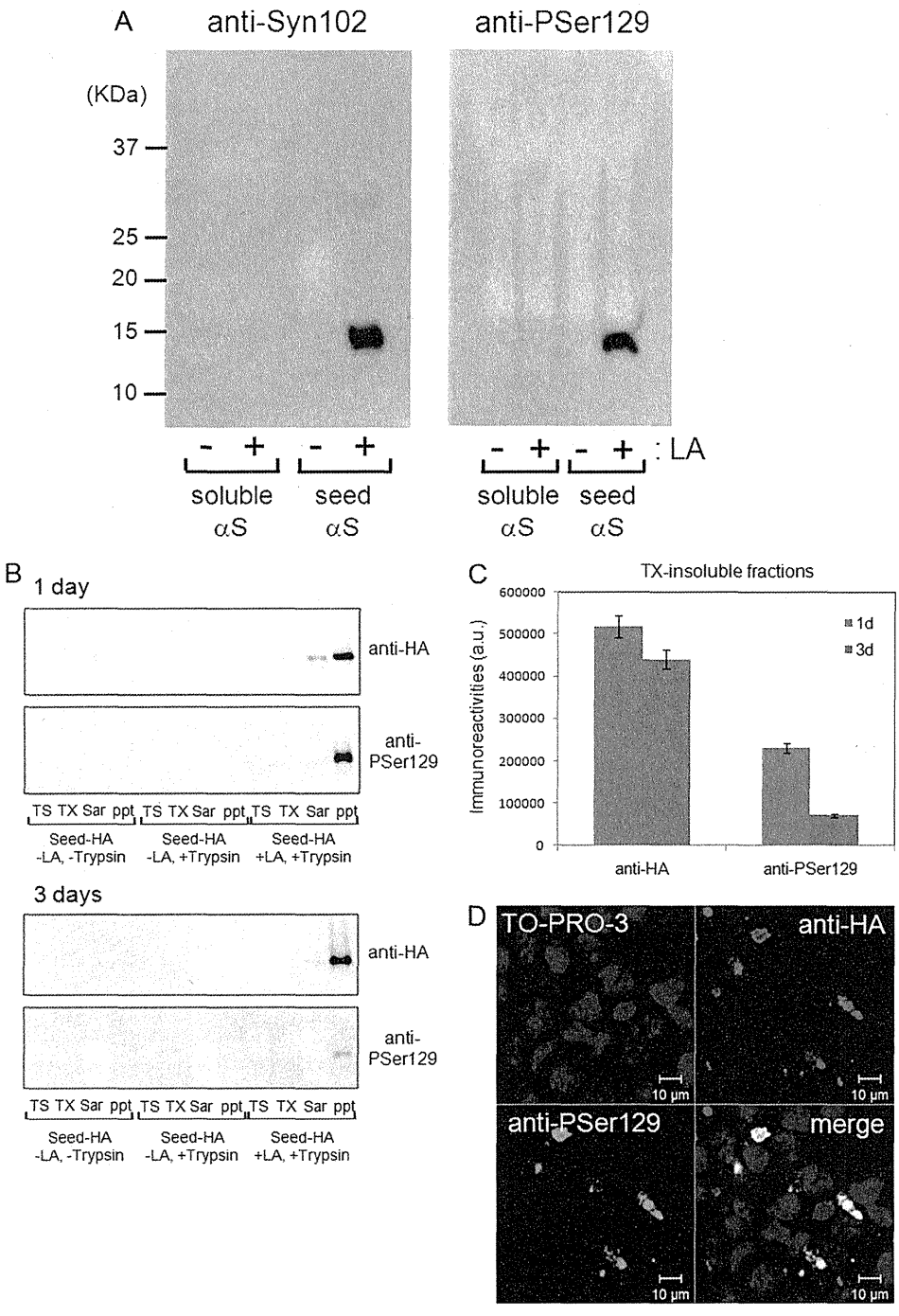

FIGURE 1. **Introduction of seed α-syn into cultured cells with Lipofectamine reagent.** *A*, purified recombinant α-syn (soluble form; 2 μg) and filaments (2 μg) were sonicated and then incubated with LA. The protein-LA complexes were dispersed in Opti-MEM and added to SH-SY5Y cells. After 14 h of culture, the cells were collected and sonicated in SDS sample buffer. After boiling, the samples were analyzed by immunoblotting with a phosphorylation-dependent anti-α-syn Ser(P)^{129} (*PSer129*) (*right*) or a phosphorylation-independent antibody, Syn102 (*left*). *B* and *C*, carboxyl-terminally HA-tagged α-syn fibril seeds (*Seed-HA*) were transduced into cells by the use of LA. After incubation for 1 day (*1d*) or 3 days (*3d*), cells were harvested with or without trypsin, and proteins were differentially extracted from the cells with Tris-HCl (*TS*), Triton X-100 (*TX*), and Sarkosyl (*Sar*), leaving the pellet (*ppt*). Immunoblot analyses of lysates using anti-HA and anti-Ser(P)^{129} are shown. The immunoreactive band positive for anti-HA or anti-Ser(P)^{129} in the Triton X-100-insoluble fraction was quantified. The results are expressed as means ± S.E. ($n = 3$). *D*, confocal laser microscopic analysis of cells treated with Seed-HA in the presence of LA. Cells were transduced with 2 μg of Seed-HA using 5 μl of LA. After a 48-h incubation, cells were fixed and immunostained with anti-Ser(P)^{129} (*green*) and anti-HA (*red*) and counterstained with TO-PRO-3 (*blue*).

fected with pcDNA3-α-syn (1 μg) and GFP-CL1 (0.3 μg) using FuGENE6 and then transfected with Seed αS were grown on coverslips for 2 days or treated with 20 μM MG132 for 6 h (19). These cells were analyzed using a laser-scanning confocal fluorescence microscope (LSM5Pascal, Carl Zeiss).

Statistical Analysis—The *p* values for the description of the statistical significance of differences were calculated by means of the unpaired, two-tailed Student's *t* test using GraphPad Prism 4 software (GraphPad Software).

RESULTS

Introduction of Seed α-Syn into Cultured Cells Using Lipofectamine Reagent—Cellular overexpression of α-syn by itself does not lead to fibrillization of α-syn in a form that resembles Lewy bodies. This prompted us to examine whether or not introduction of preformed aggregation seeds of α-syn (Seed αS) would elicit fibril formation. To introduce Seed αS into SH-SY5Y cells in a non-invasive manner, we tried several reagents used for transporting proteins or plasmid DNA into cells and found that LA, a cationic gene introducer, enables the introduction of Seed αS into SH-SY5Y cells. We were not able to detect any introduced α-syn monomer or fibrils following the simple addition of protein preparations to the culture medium, notwithstanding a previous report on this approach (20). The insoluble α-syn formed following LA-mediated Seed αS introduction was detected as buffer-insoluble α-syn in cell lysates (Fig. 1*A*). The insoluble α-syn was phosphorylated at Ser^{129} upon introduction into cells (Fig. 1*A*), indicating that Seed αS was incorporated in cells and phosphorylated intracellularly. Cells were harvested in the presence of trypsin to digest extracellular cell-associated α-syn fibrils. The optimal ratio of LA to Seed αS was about 5 μl to 2 μg of protein in 6-well plates. This treatment effectively introduced Seed αS not only into SH-SY5Y cells but also into several other types of cells examined, including Chinese hamster ovary cells and human embryonic kidney 293T cells (data not shown). In sharp contrast, soluble α-syn (either monomeric or oligomeric forms) was not introduced into the

cells by the same treatment (Figs. 1*A* and 4), suggesting that the LA treatment works exclusively for the internalization of insoluble α-syn aggregates.

These results strongly suggest that α-syn fibrils are incorporated with the aid of LA but do not exclude the possibility that extracellular α-syn fibrils may induce aggregation of endogenous α-syn without incorporation. To confirm that the extracellular α-syn fibril seeds are internalized into cells by LA, we performed the transduction of preformed carboxyl-terminally HA-tagged α-syn fibril seeds (Seed-HA) instead of non-tagged

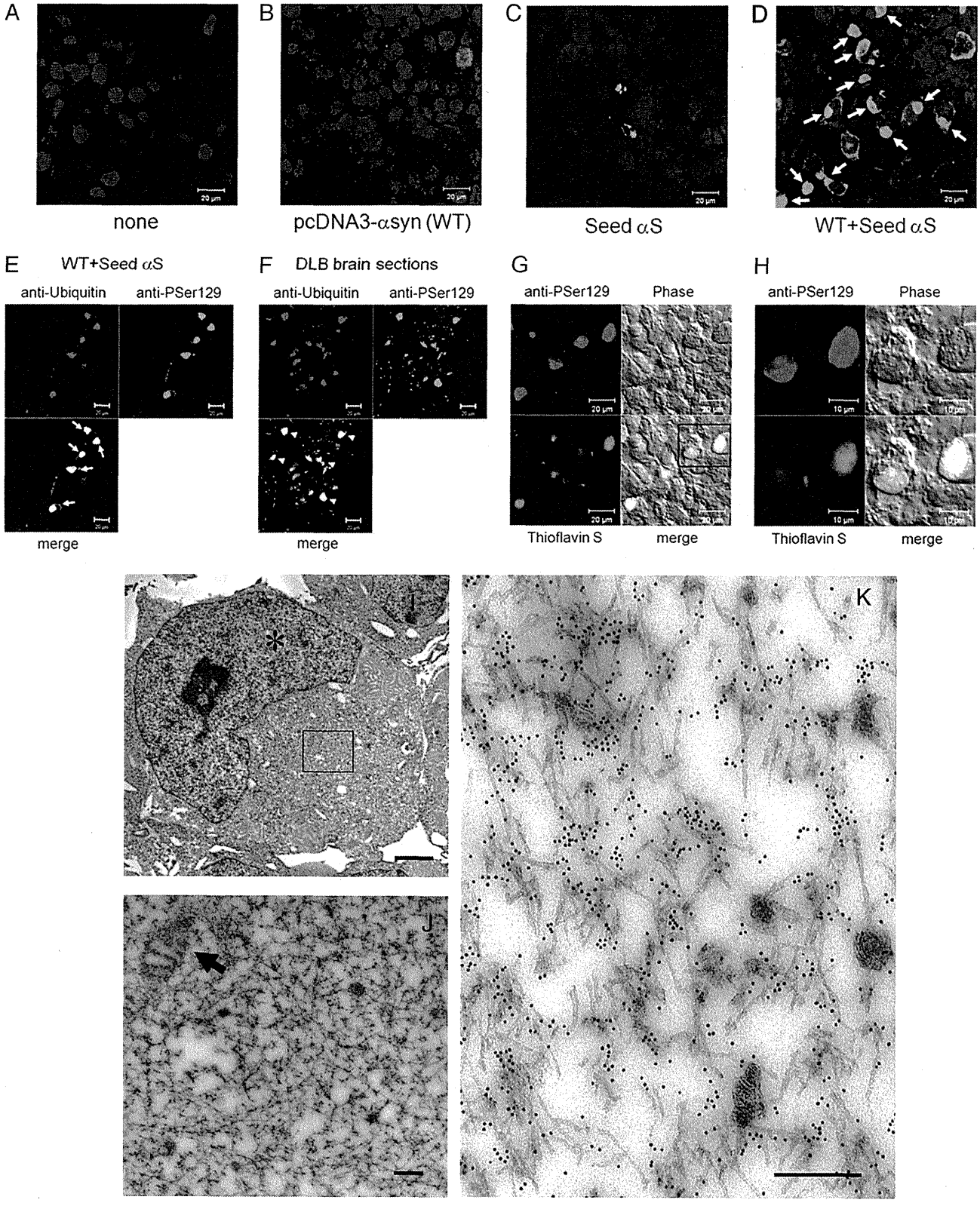

α-syn seeds. As shown in Fig. 1, *B* and *C*, time course experiments revealed that Seed-HA was also incorporated into cells in the presence of LA and could be detected with both anti-HA antibody and a phospho-α-syn-specific antibody (anti-Ser(P)^{129}), even 3 days after infection. Confocal microscopic analyses also indicated that Seed-HA was phosphorylated at Ser^{129} intracellularly. All anti-Ser(P)^{129}-positive dotlike structures were also stained with anti-HA, indicating that no endogenously phosphorylated α-syn aggregates are present in the cells (Fig. 1*D* and supplemental Fig. S1*C*).

Establishment of a Cell Culture Model for Nucleation-dependent Polymerization of α-Syn—Although introduction of the seed α-syn into cells was accompanied with phosphorylation, no further dramatic change was observed. Because the level of endogenous α-syn was relatively low in SH-SY5Y cells, we introduced non-tagged or HA-tagged seeds into cells transiently overexpressing α-syn. After 3 days of culture, immunocytochemistry for α-syn revealed a diffuse (Fig. 2*B*) or dotlike (Fig. 2*C*) pattern of cytoplasmic labeling by anti-Ser(P)^{129} in cells transfected with wild-type α-syn without seeds or in non-overexpressing cells with Seed αS, respectively. Surprisingly, however, in cells transfected with both pcDNA3-α-syn and Seed αS, we observed abundant round inclusions that occupied the cytoplasm and displaced the nucleus, with morphology highly reminiscent of cortical-type Lewy bodies observed in human brain (Fig. 2*D*). The size of the α-syn-positive inclusions was ~10 μm in diameter (Fig. 2*D*), which is similar to that of the Lewy bodies detected in the brains of patients with dementia with Lewy bodies. Similarly, when cells expressing α-syn were transfected with Seed-HA, abundant phosphorylated α-syn-positive cells were also detected (supplemental Fig. S1*D*).

We next examined the status of ubiquitin, which is positive in most types of intracellular filamentous inclusions, including Lewy bodies, in neurodegenerative disease brains. As shown in Fig. 2*E*, we found that almost all intracellular inclusions labeled with anti-Ser(P)^{129} were also positive for ubiquitin, as is the case for Lewy bodies in the cortex of human DLB brain (Fig. 2*F*). Furthermore, the juxtanuclear Ser(P)^{129}-positive, Lewy body-like inclusions were also positively labeled with thioflavin S, a fluorescent dye that specifically intercalates within structures rich in β-pleated sheet conformation (Fig. 2, *G* and *H*), indicating that the inclusions contain β-sheet-rich filamentous aggregates. Electron microscopic analysis of cells transfected with both wild-type α-syn and the seeds revealed that the inclusions are composed of filamentous structures ~10 nm in diameter that are often covered with granular materials (Fig. 2, *I* and *J*). The filamentous structures were randomly oriented within the cytoplasm of these cells, forming a meshwork-like profile, and were frequently intermingled with mitochondria (Fig. 2, *I* and *J*), being highly reminiscent of human cortical Lewy bodies. Immunoelectron microscopy showed that the filaments were densely decorated with anti-Ser(P)^{129} (Fig. 2*K*), demonstrating that they were composed of phosphorylated α-syn.

To biochemically validate this cellular model and to investigate further the molecular mechanisms underlying nucleation-dependent aggregation within cells, we differentially extracted α-syn from these cells using detergents of various strengths and analyzed the extracts by immunoblotting with anti-Syn102 and -Ser(P)^{129} antibodies. The levels of α-syn in the Sarkosyl-soluble and -insoluble fractions (total α-syn and α-syn phosphorylated at Ser^{129}, respectively) were dramatically increased in cells transfected with both wild-type α-syn and the seeds (*WT + Seed αS* in Fig. 3, *A* and *B*). To distinguish endogenous α-syn from exogenous α-syn fibrils, we used LA to transduce Seed-HA into cells overexpressing α-syn. Immunoblot analyses of these cells showed that HA-tagged α-syn with slower mobility than non-tagged α-syn was detected in the Sarkosyl-insoluble pellets as phosphorylated forms by anti-HA and anti-Ser(P)^{129} antibodies in cells treated with Seed-HA + LA (Fig. 3, *C–E*). Interestingly, in cells expressing α-syn (WT) treated with Seed-HA + LA, much more abundant non-tagged α-syn was detected in the Triton X-100- and Sarkosyl-insoluble fractions as phosphorylated forms with a smaller amount of the HA-α-syn. We also performed a dose dependence experiment with Seed-HA in cells expressing α-syn. As shown in supplemental Fig. S2, immunoreactive levels of Triton X-100-insoluble phosphorylated α-syn increased in parallel with an increase in the amount of Seed-HA. Furthermore, we tested whether Tau protein forms intracellular aggregates in the presence of α-syn seeds instead of Tau seeds. We found that Tau was not aggregated with Seed-HA, confirming that intracellular aggregate formation of soluble α-syn is specific to and dependent on fibril seeds of the same protein (supplemental Fig. S3). This nucleation-dependent polymerization of α-syn in cells was greater at 3 days than at 1 day after transduction of the seeds (Fig. 3*F*).

Negative stain electron microscopic observation of Sarkosyl-insoluble fractions of the cells harboring inclusions revealed anti-Syn102 and Ser(P)^{129}-positive filaments of ~5–10-nm width (Fig. 3, *G* and *H*) that are highly reminiscent of those derived from human α-synucleinopathy brains (21). Such filaments were never detected in the Sarkosyl-insoluble fraction of cells solely overexpressing α-syn (data not shown). These results indicated that the biochemical characteristics of α-syn accumulated in cells forming the Lewy body-like inclusions

FIGURE 2. **Confocal laser and electron microscopic analyses of α-syn inclusions in plasmid-derived α-syn-expressing cells treated with seed α-syn.** *A–D*, confocal laser microscopic analyses of control SH-SY5Y cells transfected with pcDNA3 vector and Lipofectamine alone (*A*), cells transfected with pcDNA3-α-syn (*WT*) (*B*), cells transduced with the seed α-syn (*Seed αS*) (*C*), and cells transfected with both pcDNA3-α-syn and Seed αS (*WT + Seed αS*) (*D*), immunostained with anti-Ser(P)^{129} (*green*), and counterstained with TO-PRO-3 (*blue*). The *arrows* indicate cytoplasmic round inclusions stained with anti-Ser(P)^{129} (*PSer129*). *Scale bars*, 20 μm. *E–F*, comparison of confocal images of cells transfected with both α-syn plasmid and Seed αS (*E*) and tissue sections from DLB brains (*F*) using anti-Ser(P)^{129} (*green*) and anti-ubiquitin antibodies (*red*). Cytoplasmic inclusions in transfected cells (*arrows*) are positive for ubiquitin, like Lewy bodies (*arrowheads*) in DLB brains. *Scale bars*, 20 μm. *G* and *H*, confocal microscopic images of cells transfected with both pcDNA3-α-syn and Seed αS. Cells were stained with 0.05% Thioflavin S (*green*) and anti-Ser(P)^{129} antibody (*red*). The *boxed area* on the *left* is shown in the *right panel*. *Scale bars*, 20 μm on the *left* and 10 μm on the *right*. *I* and *J*, electron microscopic analyses of cells transfected with both pcDNA3-α-syn and Seed αS. High magnification of the boxed area in *I* is shown in *J*. An *asterisk* or *arrow* indicates a nucleus or mitochondrion, respectively. *Scale bars*, 2 μm in *I* and 200 nm in *J*. *K*, immunoelectron microscopic observation of cells transfected with both pcDNA3-α-syn and Seed αS using a polyclonal antibody against phosphorylated Ser^{129} of α-syn. *Scale bar*, 200 nm.

were very similar to those of α-syn deposited in the brains of patients with α-synucleinopathies, including PD and DLB.

Because the idea has been gaining ground that transient oligomers, rather than mature fibrils, are responsible for cytotoxicity, we examined whether soluble oligomers could be introduced into cells in the same manner as fibril seeds by means of LA treatment and whether they could function as seeds for intracellular α-syn aggregate formation. As shown in Fig. 4, *A* and *B*, we purified stable α-syn oligomers from recombinant α-syn treated with exifone, an inhibitor of *in vitro* α-syn aggregation, which is thought to inhibit filament formation of α-syn by stabilizing SDS-resistant soluble oligomers (22, 23). Then cells expressing α-syn or mock plasmid were treated with a mixture of the oligomer fraction (5 μg) and LA and incubated for 3 days. Immunoblot analyses of lysates of these cells did not detect any SDS-resistant soluble oligomeric α-syn, and the levels of phosphorylated α-syn in the Sarkosyl-soluble and -insoluble fractions showed no increase (Fig. 4, *C* and *D*). On the other hand, we observed phosphorylated and deposited α-syn in the Sarkosyl-soluble and -insoluble fractions in cells expressing α-syn treated with Seed αS (Fig. 4, *C* and *D*). These results showed that SDS-resistant soluble oligomer of α-syn could not be introduced into cultured cells in the same manner as monomeric α-syn and/or could not function as seeds for intracellular α-syn aggregation.

Mutagenic Analysis of Nucleation-dependent Assembly of α-Syn—To investigate further the nucleation-dependent polymerization of α-syn, we analyzed the polymerization of α-syn mutated or truncated at various residues or subdomains that are believed to be crucial for its aggregation. Overexpression of A53T familial Parkinson mutant α-syn, which is readily fibrillogenic *in vitro*, in the presence of Seed αS moderately increased the accumulation and phosphorylation of α-syn in the Sarkosyl-soluble and insolu-

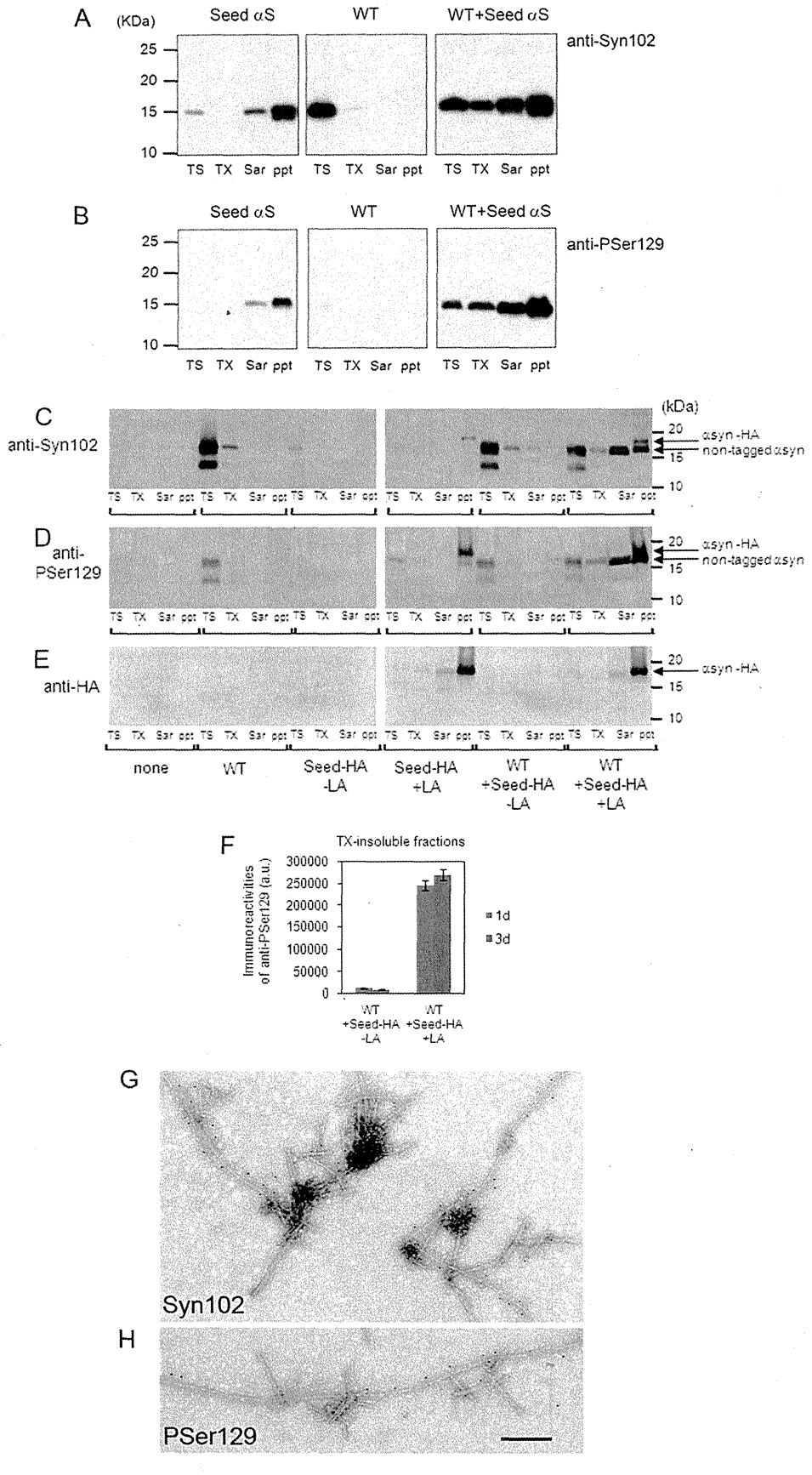

ble fractions compared with those in cells with wild-type α-syn expression and Seed αS (Fig. 5, *A* and *B*). In contrast, overexpression of Δ11 mutant α-syn, an assembly-incompetent mutant lacking residues 73–83, which have been shown to be essential for fibril formation of α-syn (24), elicited neither deposition nor phosphorylation of α-syn. We next introduced α-syn into SH-SY5Y cells expressing S129A mutant α-syn and observed slightly lower levels of Sarkosyl-insoluble α-syn compared with those in cells with wild-type α-syn expression and Seed αS. However, the frequency of inclusion bodies observed in seed-transduced cells expressing S129A was similar to that in seed-transfected cells expressing wild-type α-syn (data not shown), suggesting that phosphorylation at Ser^{129} is not required for the nucleation-dependent polymerization of α-syn within cells.

Nucleation-dependent Intracellular Polymerization of α-Syn Elicits Neurotoxicity and Cell Death—SH-SY5Y cells overexpressing α-syn started to show marked clumping suggestive of cellular degeneration and death by ~48 h after introduction of seeds (Fig. 6*B*). Quantitative analysis of cell death by a lactate dehydrogenase (LDH) release assay at 72 h after introduction of Seed αS showed that cells overexpressing wild-type, A30P, A53T, or S129A α-syn released ~30% of total LDH from total cell lysate, whereas only ~12% of LDH was released from cells expressing Δ11 mutant α-syn, which lacks polymerization ability. In control cells transfected with empty vector or pcDNA3-α-syn followed by treatment with Lipofectamine without seeds, only ~7% of LDH was released (Fig. 6*C*). These results suggest a close correlation between the seed-dependent aggregation of α-syn and cell death. However, the dying cells transfected with fibrillization-competent α-syn and seeds did not show typical morphological changes of apoptosis (*e.g.* nuclear fragmentation, positive TUNEL staining (supplemental Fig. S4*A*), or activation of caspase-3 (supplemental Fig. S4*B*)), suggesting that they did not undergo typical apoptotic cell death, despite a previous report that exposure to neuron-derived extracellular α-syn may cause apoptosis (25).

Impairment of Proteasome Activity in Cells with Intracellular Aggregates of α-Syn—Because α-syn is ubiquitinated in the brains of patients with α-synucleinopathies (26) and inhibition of ubiquitin-proteasome systems by aggregates of proteins with expanded polyglutamine tracts has been reported (27), we analyzed the ubiquitination state of cellular proteins in α-syn aggregate-forming cells and compared the pattern with that in cells treated with a proteasome inhibitor, MG132. A Sarkosyl-soluble fraction of seed-transduced cells expressing wild-type α-syn and harboring abundant inclusions showed increased levels of ubiquitin-positive staining, which was similar in pattern to that observed in cells treated with MG132 (Fig. 6*D*). Because this pattern suggested an impairment of the ubiquitin-proteasome system, we directly analyzed the proteasome activity of α-syn inclusion-forming cells using a specific fluorescent peptide substrate, benzyloxycarbonyl-Leu-Leu-Glu-7-amido-4-methylcoumarin, that emits fluorescence following proteasomal digestion and confirmed that proteasome activity was significantly reduced in these cells as well as in cells treated with 20 μM MG132 for 4 h (Fig. 6*E*). We further examined the suppression of proteasome activity using CL1, a short degron that has been reported to be an effective proteasome degradation signal (28) and whose fusion protein with green fluorescent protein (GFP-CL1) has been used as a reporter for inhibition of proteasomal activity by intracellular polyglutamine aggregates (27) and intracellular α-syn (19). To examine if intracellular α-syn inclusions affected proteasomal activity, SH-SY5Y cells were transfected with both wild-type α-syn and GFP-CL1, followed by the introduction of Seed αS. Fluorescent signals of GFP were scarcely detected in control cells transfected with GFP-CL1 alone (Fig. 6*F*, *none*) but were markedly increased upon treatment with proteasome inhibitor MG132 (Fig. 6*F*, *MG132*), confirming that GFP-CL1 was effectively degraded by proteasome. Strikingly elevated GFP signals were detected in cells forming α-syn inclusions (Fig. 6*F*, *WT + Seed αS*) compared with those in control cells (Fig. 6*F*, *none* or *WT*), and GFP-CL1 and deposits of phosphorylated α-syn were co-localized within these cells (*arrowheads*). These results strongly suggest that proteasome activity is impaired in cells harboring α-syn inclusions elicited by the introduction of Seed αS.

Small Molecular Inhibitors of Amyloid Filament Formation Protect against Cell Death Induced by Seed-dependent α-Syn Polymerization—We have previously shown that several classes of small molecular compounds inhibit amyloid filament formation of α-syn, Tau, and Aβ *in vitro* (17, 23). These observations prompted us to test whether these inhibitors exert a protective effect against death of SH-SY5Y cells mediated by the nucleation-dependent polymerization of α-syn. Fig. 7*A* shows the effects of three polyphenol compounds, exifone, gossypetin, and quercetin, and a rifamycin compound, rifampicin, added to the culture media at a final concentration of 20 or 60 μM. Remarkably, all of these compounds blocked cell death, with gossypetin being the most effective. Our previous *in vitro* studies elucidated that several polyphenols, including gossypetin and exifone, inhibit α-syn assembly and that SDS-stable, noncytotoxic soluble α-syn oligomers are formed in their presence (23), suggesting that such polyphenols may inhibit filament formation of α-syn by stabilizing soluble, prefibrillar intermediates. Gossypetin or exifone might suppress intracellular α-syn aggregate formation by stabilizing such soluble intermediates in cultured cells as well. Immunoblot analysis

FIGURE 3. **Immunoblot and immunoelectron microscopic analyses of intracellular α-syn aggregates in cultured cells.** *A* and *B*, immunoblot analysis of α-syn in cells treated with Seed αS alone (*Seed αS*), pcDNA3-α-syn alone (*WT*), or both WT and Seed αS (*WT + Seed αS*). Proteins were differentially extracted from the cells with Tris-HCl (*TS*), Triton X-100 (*TX*), and Sarkosyl (*Sar*), leaving the pellet (*ppt*). Blots were probed using anti-α-syn (Syn102) (*A*) and anti-$Ser(P)^{129}$ (*PSer129*) (*B*). *C–F*, immunoblot analysis of proteins differentially extracted from mock (none) or cells transfected with pcDNA3-α-syn (*WT*), cells transduced with Seed-HA with (*Seed-HA + LA*) or without LA treatment (*Seed-HA − LA*), and cells overexpressing α-syn treated with Seed-HA with (*WT + Seed-HA + LA*) or without LA treatment (*WT + Seed-HA − LA*). Immunoreactivity of phosphorylated α-syn in the Triton X-100-insoluble fraction was quantified using anti-$Ser(P)^{129}$, and the results are expressed as means ± S.E. ($n = 3$), as shown in *F*. a.u., arbitrary unit. *G* and *H*, immunoelectron microscopy of α-syn filaments extracted from transfected cells. SH-SY5Y cells were transfected with both pcDNA3-α-syn and Seed αS. Sarkosyl-insoluble fraction was prepared from the cells, and the filaments were immunolabeled with anti-Syn102 (*G*) or $Ser(P)^{129}$ (*H*) antibody. *Scale bar*, 200 nm. *1d* and *3d*, 1 and 3 days, respectively.

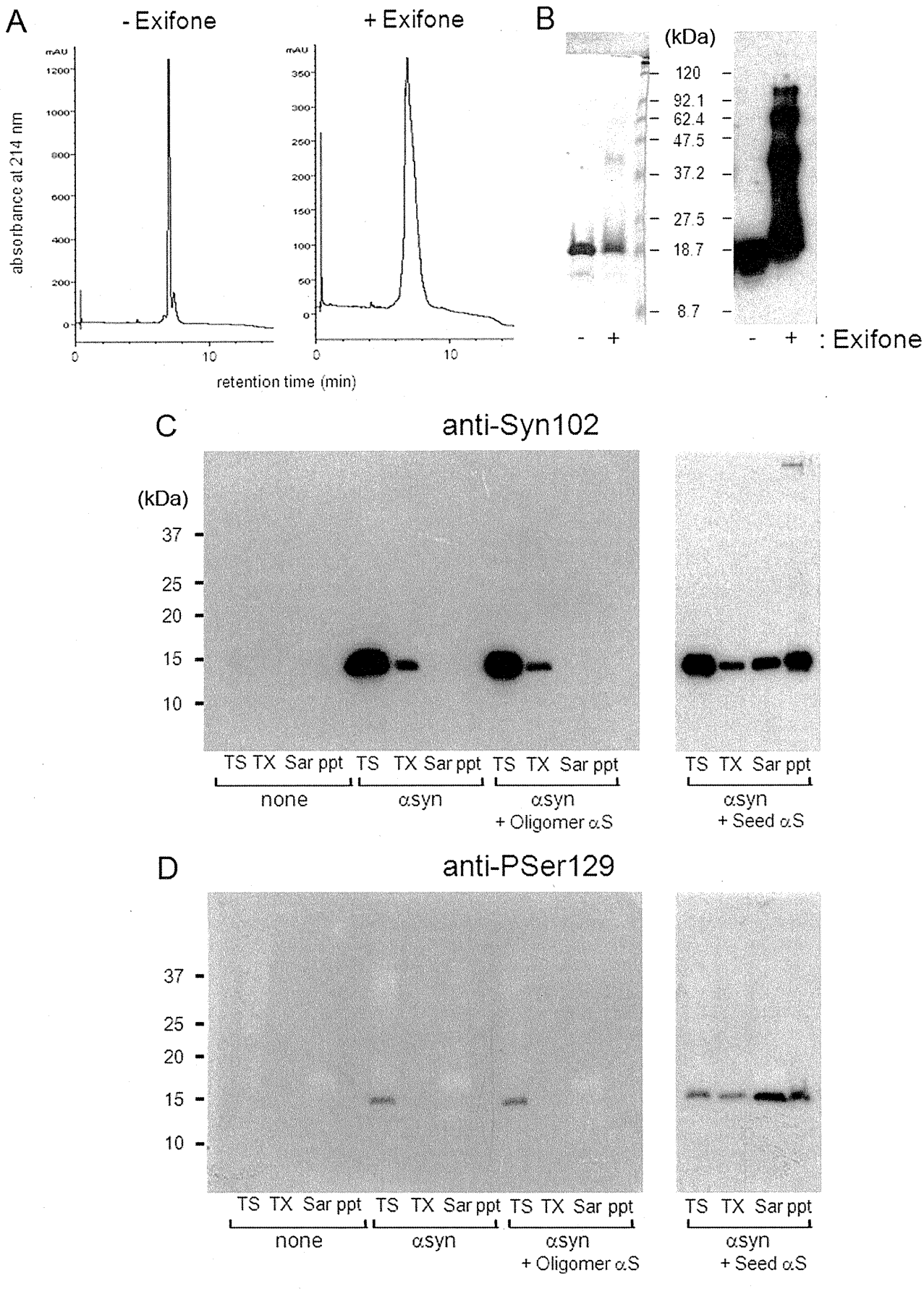
A
- Exifone
+ Exifone
mAU
absorbance at 214 nm
retention time (min)
B
(kDa)
120
92.1
62.4
47.5
37.2
27.5
18.7
8.7
- + - + : Exifone
C
anti-Syn102
(kDa)
37
25
20
15
10
TS TX Sar ppt TS TX Sar ppt TS TX Sar ppt
none
αsyn
αsyn
+ Oligomer αS
TS TX Sar ppt
αsyn
+ Seed αS
D
anti-PSer129
37
25
20
15
10
TS TX Sar ppt TS TX Sar ppt TS TX Sar ppt
none
αsyn
αsyn
+ Oligomer αS
TS TX Sar ppt
αsyn
+ Seed αS

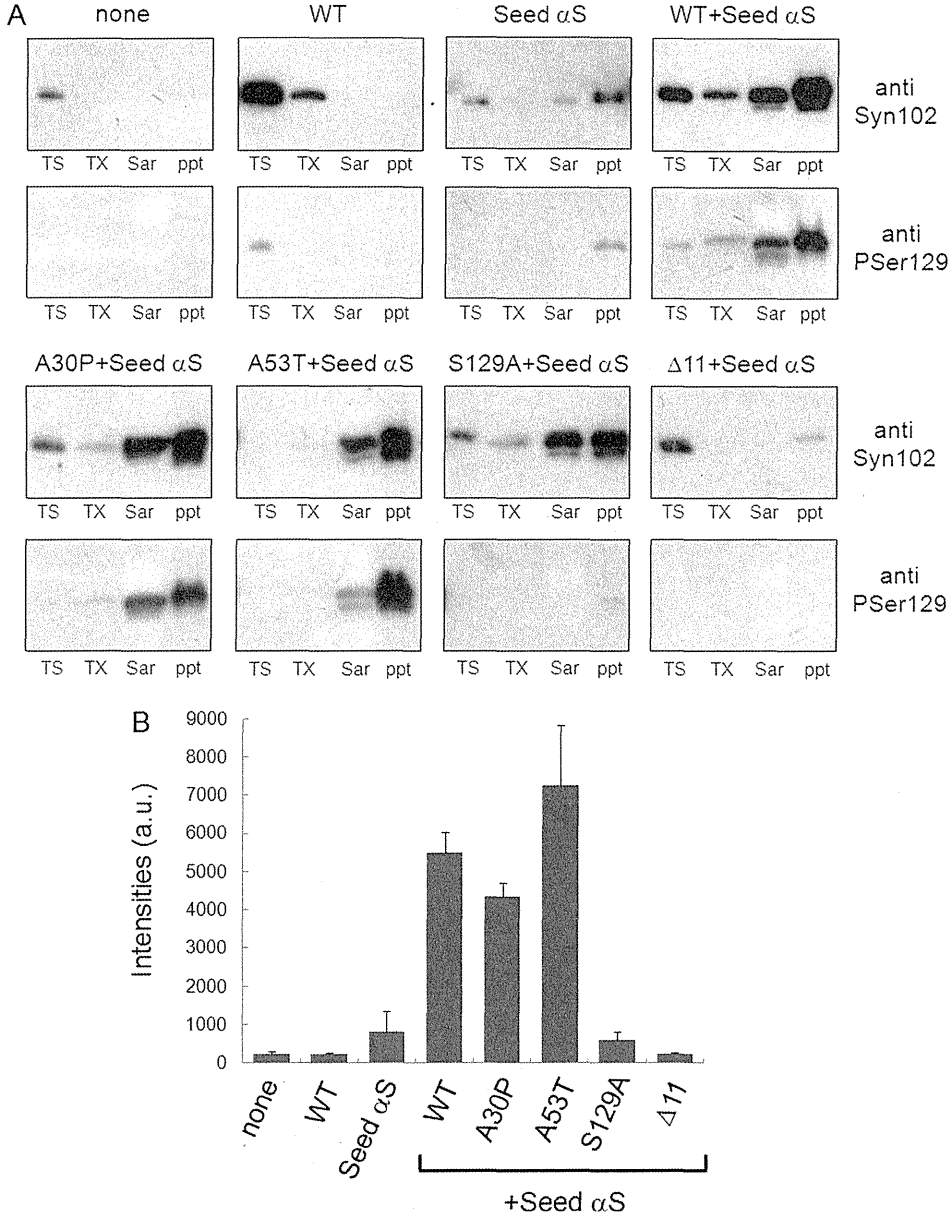

FIGURE 5. **Effects of α-syn mutations on intracellular deposition.** Immunoblot analysis of α-syn in cells transfected with pcDNA3-α-syn alone (*WT*), Seed αS alone (*Seed αS*), both WT and Seed αS (*WT + Seed αS*), and non-treated control cells (*none*). Cells overexpressing familial PD-linked A30P or A53T polymerization-deficient Δ11 mutant α-syn followed by transfection with Seed αS were also analyzed. Proteins were extracted differentially with Tris-HCl (*TS*), Triton-X (*TX*), and Sarkosyl (*Sar*), leaving the pellet (*ppt*), and immunoblotting was done with anti-Syn102 and Ser(P)^{129} (*PSer129*). The Ser(P)^{129}-immunoreactive bands detected in Sarkosyl-soluble and -insoluble fractions from each cell type shown in *A* were quantified (*B*). The results are expressed as means +S.E. (*error bars*) ($n = 3$). a.u., arbitrary unit.

revealed that the levels of Sarkosyl-insoluble α-syn in cells transfected with both α-syn and seeds were reduced by treatment with exifone or gossypetin compared with those in untreated cells (Fig. 7*B*), supporting the notion that these compounds entered the cytoplasm and blocked cell death by suppressing the seed-dependent polymerization of α-syn.

Cellular Models for Nucleation-dependent Polymerization of Tau—Beside α-syn, Tau is another major pathogenic protein that is deposited in degenerating neurons or glial cells in various neurodegenerative diseases, and aggregation of distinct Tau isoforms has been found in different diseases (*i.e.* deposition of three-repeat Tau isoforms in Pick's disease, four-repeat Tau isoforms in progressive supranuclear palsy and corticobasal degeneration, and both three- and four-repeat Tau isoforms in AD). It is unknown why distinct Tau isoforms deposit in different diseases. Thus, we also tried to establish a cellular model of intracellular Tau aggregate formation by transduction of Tau fibril seeds into cultured cells. First, we confirmed that expression of 3R1N or 4R1N by itself induced phosphorylation of Ser^{396}, but no aggregated form was detected in detergent-insoluble fractions (Fig. 8 and supplemental Fig. S5). Next, we tested whether introduced Tau 4R1N or 3R1N fibril seed (Seed 4R1N or 3R1N, respectively) is detectable by immunoblot analysis using anti-T46, anti-HT7, or anti-Ser(P)^{396} antibody. However, we could not detect any band in Triton X-100-insoluble fractions of cells treated with Seed Tau 4R1N or 3R1N in the presence of LA with any of these antibodies (data not shown). It seems likely that the efficiency of introduction of Tau 4R1N and 3R1N fibrils by LA treatment is very low, as compared with that of Seed αS. Then we checked whether treatment with recombinant Tau fibrils causes intracellular Tau aggregate formation in an LA-dependent manner. As shown in supplemental Fig. S5, LA treatment itself did not cause intracellular Tau deposition in cells expressing Tau 4R1N without

FIGURE 4. **α-Syn oligomers were not introduced into cultured cells.** *A* and *B*, α-Syn oligomers were prepared as described under "Experimental Procedures." Oligomeric α-syn protein incubated with (47.8 μg of protein) or without exifone (30 μg of protein) was analyzed by reversed-phase HPLC (Aquapore RP-300 column) (*A*). These samples (0.2 μg of protein of each) were also analyzed by SDS-PAGE and immunoblotted with anti-Syn102 (*B*). *C* and *D*, cells were transfected with empty plasmid (*none*) or pcDNA3-αsyn (*αsyn*) and then treated with or without α-syn oligomer (*Oligomer αS, 5 μg*) or fibrils (*Seed αS, 2 μg*). After incubation for 3 days, cells were harvested, and immunoblot analyses were performed. Proteins differentially extracted from the cells with Tris-HCl (*TS*), Triton X-100 (*TX*), Sarkosyl (*Sar*), and the pellet (ppt) were probed using anti-Syn102 (*C*) and anti-Ser(P)^{129} (*PSer129*) (*D*).

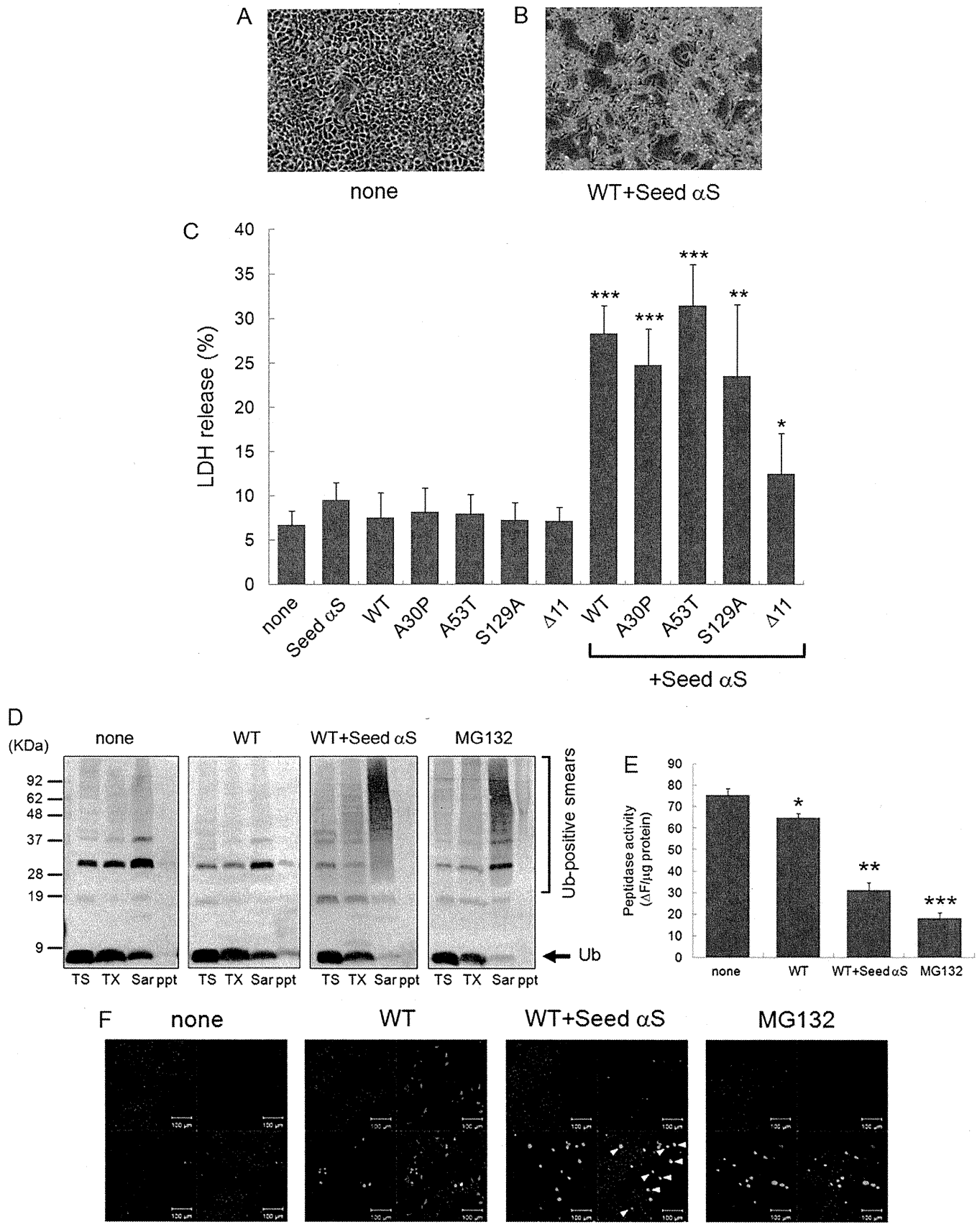
A
B
none
WT+Seed αS
C
LDH release (%)
40
35
30
25
20
15
10
5
0
***
***
***
**
*
none
Seed αS
WT
A30P
A53T
S129A
Δ11
WT
A30P
A53T
S129A
Δ11
+Seed αS
D
(KDa)
none
WT
WT+Seed αS
MG132
92
62
48
37
28
19
9
TS TX Sar ppt
TS TX Sar ppt
TS TX Sar ppt
TS TX Sar ppt
Ub-positive smears
Ub
E
Peptidase activity (ΔF/μg protein)
90
80
70
60
50
40
30
20
10
0
*
**
***
none
WT
WT+Seed αS
MG132
F
none
WT
WT+Seed αS
MG132

Seed 4R1N. Recombinant Tau 4R1N monomer in the presence of LA did not elicit the formation of intracellular Tau aggregates in these cells. On the other hand, when Seed 4R1N was added to cells expressing Tau 4R1N with LA, aggregated and phosphorylated Tau was detected in Sarkosyl-insoluble fractions by immunoblot analyses of these cell lysates using anti-HT7 or anti-Ser(P)^{396} antibody (supplemental Fig. S5 and Fig. 8). In the case of intracellular Tau 3R1N aggregate formation, the results were similar to those in the experiments using Tau 4R1N described above (data not shown).

Intracellular aggregated four- or three-repeat Tau was also found to be detected with not only anti-Ser(P)^{396} but also anti-AT100 antibody in the Sarkosyl-insoluble fraction (Fig. 8, *B* and *C*). Phosphorylated and deposited Tau was not found in the Triton X-100-insoluble fraction of Tau-expressing cells without Tau seed treatment or mock plasmid-expressing cells treated with Tau seed. In accordance with findings described earlier in this paper, these results suggested that soluble four- or three-repeat Tau expressed from the plasmid was accumulated into intracellular inclusions in the presence of small amounts of Seed 4R1N or 3R1N.

We also found that hyperphosphorylated and aggregated Tau was not detected in three-repeat Tau-expressing cells treated with Seed 4R1N (Fig. 8, *B* and *C*). On the other hand, the aggregated form of three-repeat Tau was detected in Triton X-100-insoluble fractions of three-repeat Tau-expressing cells treated with Seed 3R1N, and hyperphosphorylation at Ser^{396} and Ser^{212}/Thr^{214} was observed in fractionated samples of these cells, whereas no such bands were detected in four-repeat Tau-expressing cells treated with Seed 3R1N (Fig. 8, *B* and *C*). These results clearly showed that four-repeat Tau fibrils can be seeds for polymerization of four-repeat Tau, and three-repeat Tau fibrils can be seeds for polymerization of three-repeat Tau. Tau does not polymerize (cross-seed) in the presence of seeds of a different isoform. Similarly, no Tau aggregation was detected in Tau-expressing cells treated with α-syn fibril seeds (supplemental Fig. S3, *C* and *D*), and no α-syn aggregation was detected in α-syn-expressing cells transduced with Tau fibril seeds (data not shown). Furthermore, we observed anti-AT100 and anti-Ser(P)^{396}-positive Tau 4R1N or 3R1N filaments of ~15-nm width by negative stain electron microscopic analyses of Sarkosyl-insoluble fractions of cells transfected with both Tau plasmid and the seeds (Fig. 9, *A–D*).

Confocal microscopic analyses also showed that GFP-tagged Tau 4R1N (GFP-Tau 4R1N) is aggregated into round inclusions in the presence of Seed 4R1N together with LA (Fig. 8*E*). No inclusion-like structures were found in cells expressing GFP-Tau 4R1N (Fig. 8*D*) or in cells expressing GFP-Tau 4R1N after treatment with Seed 3R1N (data not shown). The ratio of the round aggregates to all GFP-positive transfectants was calculated to be 5.8% ± 0.8602 ($p = 0.0002$ by Student's *t* test against the value of cells expressing GFP-4R1N, $n = 5$). Significant cell death was not observed in cells containing intracellular 3R1N or 4R1N aggregates (data not shown). These results strongly suggest that proteins assemble easily into amyloid fibrils in the presence of amyloid seeds derived from the same protein but not a different protein.

DISCUSSION

Nucleation-dependent protein polymerization occurs in many well characterized physiological processes (*e.g.* microtubule assembly and actin polymerization). It is also the mechanism of amyloid fibril formation in various pathological conditions and has been confirmed to occur *in vitro* for a wide variety of extracellular amyloids, such as Aβ peptides and prion proteins (12, 13) as well as intracellular proteins, such as α-syn and Tau (29, 30, 42). Both extra- and intracellular amyloids have been well studied *in vitro*, but much less is known about the mechanisms of assembly *in vivo*. Here we report a simple and effective method to introduce polymerization seeds into cells using Lipofectamine, a widely used transfection reagent. This method enabled us to evaluate the nucleation-dependent polymerization of α-synuclein and to establish a cellular model of the neurodegeneration seen in Parkinson disease.

Lipofectamine is a reagent widely used for the transfection of DNA into eukaryotic cells through the formation of liposomes of polycationic and neutral lipids in water, based on the principle of cell fusion. Various methods, including microinjection, the calcium phosphate method, the DEAE-dextran method, electroporation, and viral transfer, have been employed to introduce substances that are not normally incorporated into eukaryotic cells under physiological conditions. Microinjection is versatile but is not efficient in experiments involving large numbers of cells, and the traumatic damage to cells hampers evaluation of cytotoxic effects. Here, we have successfully employed lipofection to introduce protein aggregates as seeds

FIGURE 6. **Cell death caused by formation of intracellular α-syn inclusions.** *A* and *B*, phase-contrast microscopy of the control cells (*A*) and cells transfected with both pcDNA3-α-syn and Seed αS (*B*) 3 days after treatment with Seed αS (20× objective). *C*, the extent of cell death of transfected cells was quantified using an LDH release assay. Cells transfected with α-syn plasmid alone (WT, A30P, A53T, S129A, or Δ11) or with both wild-type or several mutants and Seed αS were incubated, and the cell death assay was performed 3 days thereafter. The results are expressed as means + S.E. (*error bars*) ($n = 5$). *, not significant; **, $p < 0.01$; ***, $p < 0.0005$ by Student's *t* test against the value of Seed αS. *D–F*, impairment of proteasome activity caused by intracellular aggregates of α-syn. *D*, immunoblot analysis of proteins sequentially extracted from non-treated cells (*none*) and cells transfected with wild-type α-syn plasmid alone (*WT*) or with both pcDNA3-α-syn and Seed αS (*WT + Seed αS*) and cells treated with 1 μM MG132 for 16 h (MG132) using anti-ubiquitin antibody. An *arrow* indicates monomeric ubiquitin. Polyubiquitinated proteins, reflecting impairment of the proteasome activity, are observed in the Sarkosyl-soluble fraction. *TS*, Tris-soluble; *TX*, 1% Triton X-100-soluble; *Sar*, 1% Sarkosyl-soluble; *ppt*, Sarkosyl-insoluble and SDS-soluble. *E*, peptide hydrolysis activity of proteasome. Cytosol fractions of non-treated control cells (*none*), cells transfected with wild-type α-syn plasmid alone (*WT*) or with WT and Seed αS (*WT + Seed αS*), and cells treated with 20 μM MG132 for 4 h (*MG132*) were prepared and assayed using benzyloxycarbonyl-Leu-Leu-Glu-7-amido-4-methylcoumarin as a substrate. The results are expressed as means + S.E. ($n = 3$). *, $p < 0.05$; **, $p < 0.01$; ***, $p < 0.0005$ by Student's *t* test against the value of none. *F*, proteasome activity in cells having intracellular aggregates of α-syn. SH-SY5Y cells transfected with both GFP-CL1 and WT were treated with Seed αS for 2 days, fixed, and stained with anti-Ser(P)^{129}. In the staining of cells transfected with wild-type α-syn plasmid alone (*WT*), anti-Syn102 was used. As a control, untreated or MG132-treated cells were also stained and analyzed. In untreated control cells, the fluorescence of GFP was poorly detected because GFP-CL1 could be degraded by proteasome in cells. In cells treated with MG132, fluorescence was markedly increased as compared with that in untreated cells because of the inhibition of proteasome activity by MG132. Co-localized images (*arrowheads*) with both increased intensities of GFP (*green*) and the fluorescence of anti-Ser(P)^{129} (*red*) were detected in cells transfected with both WT and Seed αS (*WT + Seed αS*), indicating that the proteasome activity in these cells was inhibited.

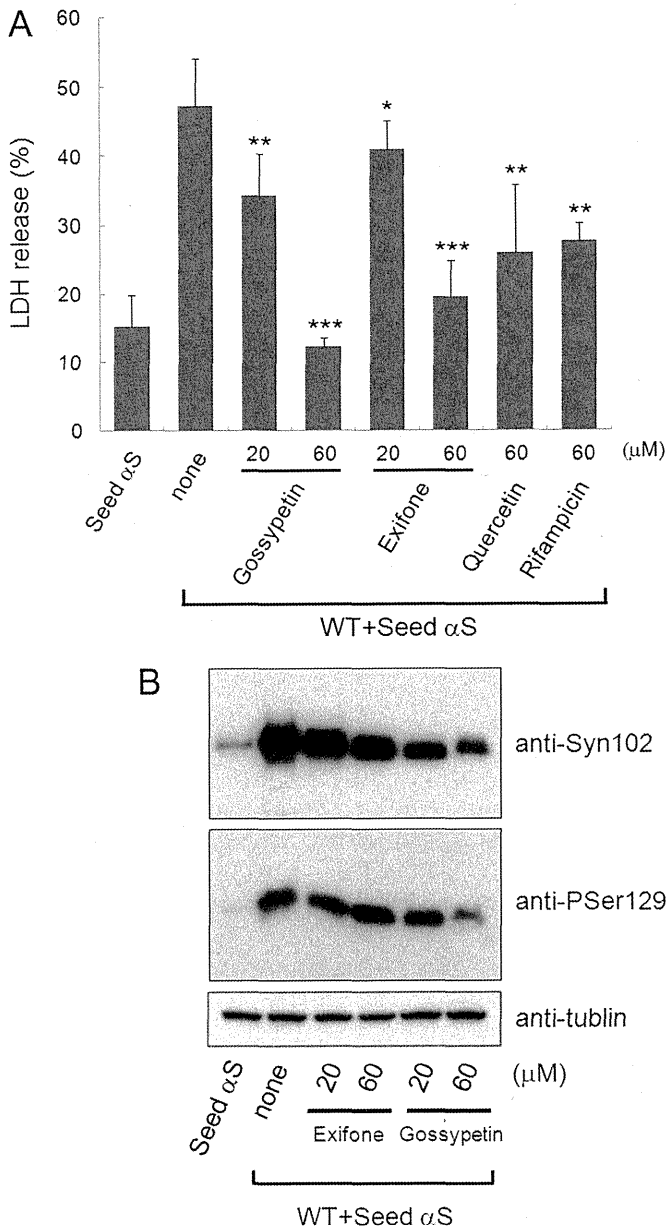

FIGURE 7. **Small molecular inhibitors of amyloid filament formation protect against cell death caused by intracellular α-syn aggregates.** *A*, the cell death of cells transfected with Seed αS and with both α-syn plasmid (*WT*) and Seed αS in the presence or absence of 20 or 60 μM gossypetin, 20 or 60 μM exifone, 60 μM quercetin, or 60 μM rifampicin was quantified by LDH release assay. The results are expressed as means ± S.E. (*error bars*) ($n = 4$). *, not significant; **, $p < 0.05$; ***, $p < 0.0005$ by Student's *t* test against the value of none. *B*, immunoblot analyses of the Sarkosyl-insoluble fraction prepared from cells transfected with Seed αS and with both WT and Seed αS in the absence or presence of exifone or gossypetin, with anti-Syn102 and anti-Ser(P)^{129} (*PSer129*) antibodies. Doubly transfected cells were treated with 20 or 60 μM exifone or gossypetin 2 h after transfection of Seed αS and cultured for 3 days in the presence of polyphenols. Tubulin-α loading controls are also shown.

for amyloid fibril formation (patent pending for the United States (12/086124), the European Union (06834541.2), and Japan (2007-549210)). The reason why Lipofectamine could specifically incorporate Seed αS but not soluble α-syn into cells is unknown. However, one possibility is that aggregated α-syn with an ordered filamentous structure was preferentially bound to Lipofectamine and formed a complex that could be more effectively transported into cells compared with soluble α-syn, which has a random coil structure. In line with this idea, it has been reported that yeast prion fibrils can be introduced into yeast cells (31). Recently, Luk *et al.* (32) have also reported that α-syn monomers and fibrils but not oligomers were introduced into cells by Bioporter, a cationic-liposomal protein transduction reagent.

We confirmed the incorporation of insoluble α-syn seeds into cells by detecting phosphorylation of α-syn, as has been seen in intracellular aggregates of α-syn in various neurodegenerative conditions referred to as synucleinopathies. This suggests that Seed αS introduced into cells is a good target for phosphorylation at Ser^{129}. In contrast to our results, a recent report suggested that α-syn fibrils were not phosphorylated after internalization (32). It is possible that this specific phosphorylation represents an active attempt by cells to maintain the intracellular milieu by sequestering protein species that are harmful to cells. Notably, the phosphorylation of α-syn was dramatically increased when Seed αS was introduced into cells overexpressing soluble α-syn (Fig. 3 and supplemental Figs. S1*D* and S2). The possibility therefore arises that widespread propagation of hyperphosphorylation of α-syn throughout the cytoplasm reflects the activation of a certain kinase(s) associated with conversion of soluble α-syn into the fibrillar form in the presence of Seed αS. However, further investigation is needed to elucidate the importance of phosphorylation for protein aggregation.

The significance of intracellular and extracellular protein aggregates in neurodegeneration is still a matter of debate. The present results clearly show that nucleation-dependent polymerization of amyloid-like proteins is closely related to neuronal degeneration leading to cell death. According to the seeding theory, amyloid fibrils grow rapidly, without a time lag, when seeds are exposed to an amount of amyloidogenic soluble protein that exceeds the critical concentration. Our experiments with seed-transfected SH-SY5Y cells overexpressing α-syn clearly demonstrated that this is the case in the intracellular environment. We have unequivocally demonstrated that nucleation-dependent polymerization of amyloid-like fibrils can occur inside cells, and the intracellular filament formation elicits a variety of cellular reactions, including hyperphosphorylation and compromise of the ubiquitin proteasome system. We also showed that α-syn oligomers were not introduced into cells by LA and did not function as seeds for α-syn aggregate formation in cultured cells. It has been speculated that protein fibrils, not oligomers, are spread or transmitted in recently reported *in vivo* models (25, 33).

Our study also revealed that intracellular protein aggregation is highly dependent on the species of protein fibril seeds. This important finding may explain why only certain Tau isoforms are deposited in several tauopathies, including Pick disease, progressive supranuclear palsy, and corticobasal degeneration. In this study, α-syn fibrils were shown to be unable to seed intracellular Tau aggregation, which is consistent with neuropathological reports that deposited α-syn is not markedly colocalized with Tau aggregates. Our observations strongly support a seed-dependent mechanism for the formation of the intracellular protein aggregates.

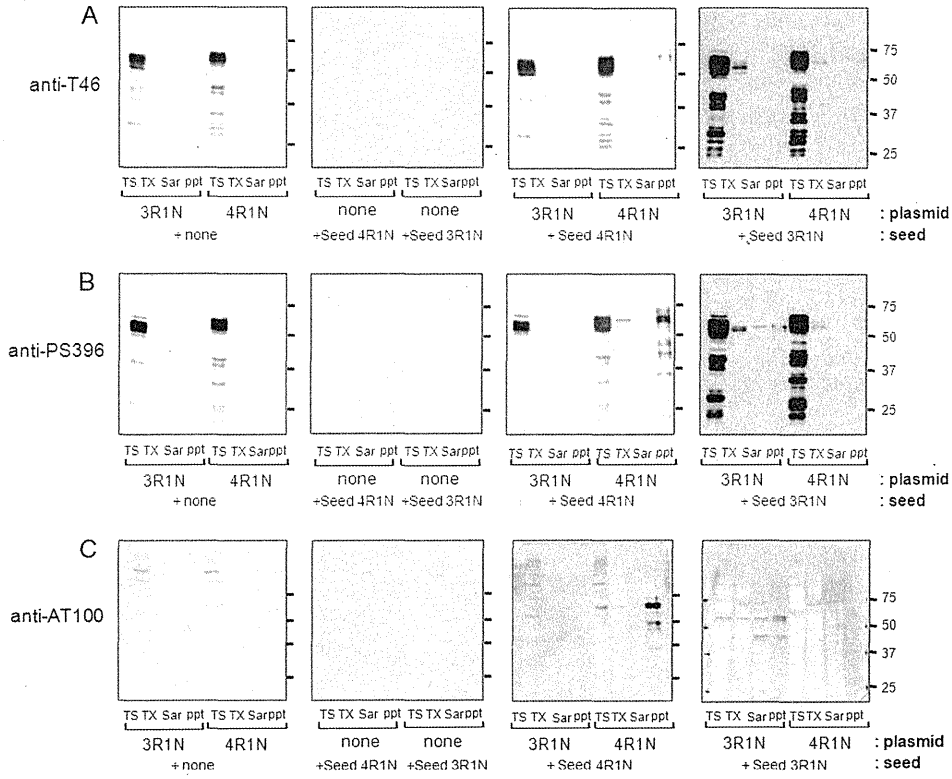

FIGURE 8. **Immunoblot analyses of intracellular Tau aggregates.** *A–C*, immunoblot analysis of Tau in cells treated with Tau fibrils alone (Seed 3R1N or Seed 4R1N), pcDNA3-Tau alone (3R1N or 4R1N), or both Seed Tau and pcDNA3-Tau. Tau proteins differentially extracted from the cells with Tris-HCl (*TS*), Triton X-100 (*TX*) and Sarkosyl (*Sar*), and the pellet (*ppt*) were probed with anti-T46 (*A*), anti-Ser(P)^{396} (*PS396*) (*B*), and anti-AT100 (*C*).

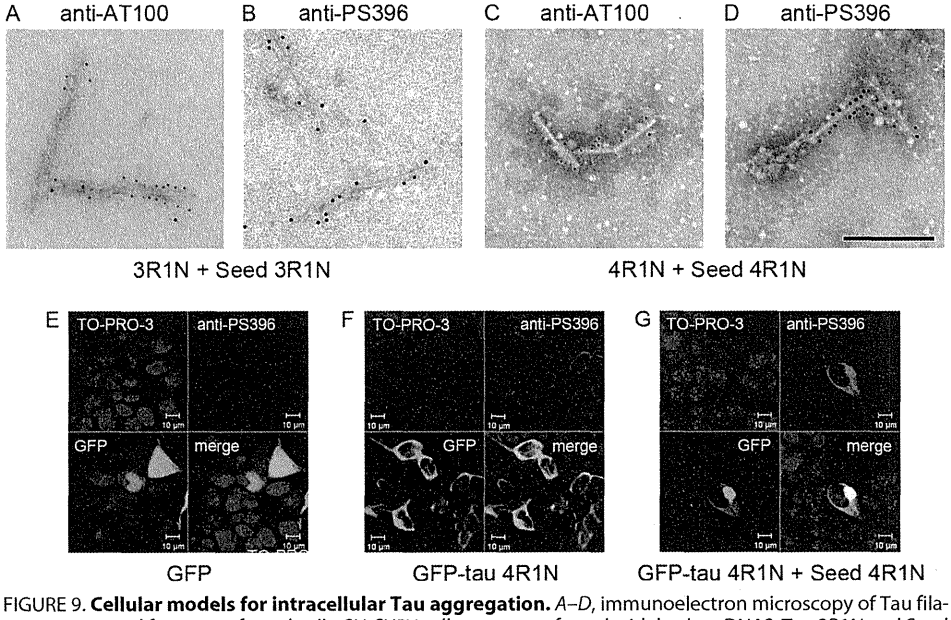

FIGURE 9. **Cellular models for intracellular Tau aggregation.** *A–D*, immunoelectron microscopy of Tau filaments extracted from transfected cells. SH-SY5Y cells were transfected with both pcDNA3-Tau 3R1N and Seed 3R1N (*A* and *B*) or pcDNA3-Tau 4R1N and Seed 4R1N (*C* and *D*). The Sarkosyl-insoluble fraction was prepared from the cells, and the filaments were immunolabeled with anti-AT100 (*A* and *C*) or anti-Ser(P)^{396} (*PS396*) (*B* and *D*) antibody. *Scale bar*, 200 nm. *E–G*, confocal laser microscopic analyses of SH-SY5Y cells transfected with pEGFP empty vector (*E*), pEGFP-Tau 4R1N (*F*), and cells transfected with both pEGFP-Tau 4R1N and Seed 4R1N (*G*), immunostained with anti-Ser(P)^{396} (*red*), and counterstained with TO-PRO-3 (*blue*). *Scale bars*, 10 μm.

Importantly, we showed that seed α-syn or Tau, an insoluble aggregate prepared from α-syn or Tau filaments, is effectively incorporated into cells by lipofection. This, in turn, suggests that high molecular weight protein aggregates or amyloid seeds shed from one cell may easily be propagated to others (*e.g.* neurons or glial cells) under pathological conditions (*e.g.* alteration in membrane permeability due to aging or virus infection, impairment of membrane function as a result of physical interaction with extracellular amyloid deposits, or abnormal membrane depolarization) that favor intracellular deposition of protein fibrils.

It remains to be clarified whether the incorporation of amyloid seeds into neurons or glial cells, as shown in this study, also occurs *in vivo*. However, some observations in AD or in transgenic animals support this possibility; apolipoprotein E (apoE) is involved in lipoprotein particle uptake mediated by cell surface receptors, and the E4 allele is the strongest genetic risk factor for AD. The apoE polypeptide has also been shown to bind Aβ (34), Tau (35), and the non-Aβ component of Alzheimer disease region of α-syn (36) and to be localized in amyloid plaques and neurofibrillary tangles in AD and prion plaques (37) in Creutzfeldt-Jakob disease. ApoE and low density lipoprotein receptor-related protein facilitate intraneuronal Aβ42 accumulation in transgenic mice (38). Furthermore, activation of both endocytic uptake and recycling of these proteins at a preclinical stage has been reported in sporadic AD and Down syndrome (39). Thus, it is strongly suggested that extracellular amyloid may be taken up into neurons by apoE and lipoprotein receptor-related protein-mediated endocytosis. Therefore, intracellular amyloid seeds composed of α-syn or Tau may also be incorporated into neurons by similar mechanisms when these seeds are released to the extracellular space after neuronal death.

It is well established that Tau protein starts to accumulate in the entorhinal region and spreads to the neocortices, closely correlating with the progression of AD (40). Similarly, accumulation of phosphorylated α-syn has been shown to start in vulnerable regions (*i.e.* limbic cortices) and to spread to the neocortices in PD or DLB. However, the mechanism of propagation of abnormal